

UNIVERSITÀ DEGLI STUDI DI VERONA

DIPARTIMENTO DI

Neuroscienze, biomedicina e movimento

SCUOLA DI DOTTORATO DI

Scienze della vita e della salute

DOTTORATO DI RICERCA IN

*Medicina biomolecolare
Curriculum: Biochimica*

CICLO XXXII

Redox regulation of STAT1 in microglia M1 activation

S.S.D. BIO/10

Coordinatore: Prof.ssa Lucia De Franceschi

Firma _____

Tutor: Prof.ssa Sofia Giovanna Mariotto

Firma _____

Co-Tutor: Dott.ssa Elena Butturini




Firma _____

Dottorando: Dott.ssa Diana Boriero

Firma _____

Quest'opera è stata rilasciata con licenza Creative Commons Attribuzione – non commerciale
Non opere derivate 3.0 Italia . Per leggere una copia della licenza visita il sito web:

<http://creativecommons.org/licenses/by-nc-nd/3.0/it/>

-  **Attribuzione** Devi riconoscere una menzione di paternità adeguata, fornire un link alla licenza e indicare se sono state effettuate delle modifiche. Puoi fare ciò in qualsiasi maniera ragionevole possibile, ma non con modalità tali da suggerire che il licenziante avalli te o il tuo utilizzo del materiale.
-  **NonCommerciale** Non puoi usare il materiale per scopi commerciali.
-  **Non opere derivate** —Se remixi, trasformi il materiale o ti basi su di esso, non puoi distribuire il materiale così modificato.

Redox regulation of STAT1 in microglia M1 activation

Diana Boriero
Tesi di Dottorato
Verona, 10 Dicembre 2019

Sommario

STAT1 è un fattore trascrizionale implicato nella regolazione di vari processi cellulari, tra cui la risposta immunitaria e l'apoptosi. Alcuni autori riportano che l'iperattivazione della via di segnale di STAT1 è coinvolta nello sviluppo della neuroinfiammazione, un processo strettamente correlato allo stress ossidativo. Nonostante il ruolo dello stress ossidativo nella patogenesi della neurodegenerazione sia già chiaramente descritto, il suo effetto sulla regolazione del signaling di STAT1 è ancora poco conosciuto.

In questo lavoro è dimostrato che lo stress ossidativo induce rapidamente l'attivazione di STAT1 in cellule BV2 di microglia murina in seguito a trattamento con H₂O₂ o ipossia. Il meccanismo molecolare della sua attivazione coinvolge la S-glutathionilazione dei residui Cys324 e Cys492 di STAT1. Questi risultati rivelano che STAT1 è una proteina redox-sensibile e che la sua attivazione in presenza di stress ossidativo coinvolge sia la fosforilazione in tirosina 701 che la S-glutathionilazione dei residui di cisteina 324 e 492.

Diversi studi riportano che l'attivazione della microglia M1 è il tratto distintivo della neuroinfiammazione e che questa contribuisce alla neuroinfiammazione e alla perdita della funzione neurologica. In questo lavoro sono analizzati i meccanismi che portano all'attivazione della microglia M1 nelle cellule BV2 in presenza di stress ossidativo, correlandola all'attivazione del fattore STAT1. Silenziando l'espressione della proteina STAT1, la transizione verso il fenotipo M1 della microglia indotta dall'ipossia è inibito, suggerendo la forte correlazione tra STAT1 e l'attivazione della microglia indotta dall'ipossia. Inoltre è qui dimostrata la capacità della microglia attivata da ipossia di indurre l'apoptosi neuronale utilizzando un modello di cross-talk *in vitro* tra le linee cellulari BV2 e SH-SY5Y.

Infine, è stata verificata l'abilità della miricetina, un flavonoide con nota attività specifica anti-STAT1, di inibire l'attivazione della microglia indotta da ipossia, prevenendo la morte neuronale nel modello di cross-talk cellulare.

Abstract

STAT1 is a transcription factor implicated in the regulation of various cell processes such as immune response and apoptosis. Some authors report that hyper-activation of STAT1 signaling is involved in the development of neuroinflammation, a process closely related to oxidative stress. Although the role of oxidative-stress in neuroinflammation and in the pathogenesis of neurodegenerative disorders is clearly described, its influence in the regulation of STAT1 pathway is poorly understood.

Herein, it is demonstrated that oxidative stress induces rapid activation of STAT1 signaling in murine microglia BV2 cells using H₂O₂ and hypoxia treatment. The molecular mechanism of its activation is related to S-glutathionylation on Cys324 and Cys492 residues of STAT1. These results reveal that STAT1 is a redox-sensitive protein and that its activation involves both tyrosine phosphorylation and S-glutathionylation under oxidative stress condition.

Several studies report that microglia M1 activation is the hallmark of neuroinflammation and contributes to neurodegeneration and loss of neurological function. Here, the mechanisms that drive M1 microglia activation in BV2 cells under hypoxic stimulus have been analysed and correlate it to STAT1 activation. Silencing of STAT1 protein expression, hypoxia-induced M1 microglia phenotype is counteracted suggesting the strong link between STAT1 and microglia activation triggered by hypoxia.

Moreover, the ability of hypoxia-activated microglia to induce neuronal apoptosis is shown using *in vitro* cross-talk model between BV2 and SH-SY5Y cell lines. Finally, it is revealed that a specific anti-STAT1 flavonoid myricetin is able to counteract microglia activation under hypoxia preventing neuronal death in the cross-talk cellular model.

Index

1. Introduction	7
1.1. Signal Transducer and Activator of Transcription 1	7
1.1.1. STAT1 structure	8
1.1.2. STAT1 signalling pathway	10
1.1.3. Regulatory post-translational modifications of STAT1	16
1.2. Oxidative stress and S-glutathionylation	17
1.2.1. Cellular redox state and ROS homeostasis	17
1.2.2. The glutathione and the redox couple GSH/GSSG	18
1.2.3. Protein cysteinyl thiols oxidation and S-glutathionylation	20
1.3. Neuroinflammation	23
1.3.1. Microglia activation	23
2. Materials and methods	28
2.1. Reagents	28
2.2. Cell cultures	28
2.3. Cells transfection	28
2.4. Western Blot analysis	29
2.5. Electrophoretic Mobility Shift Assay (EMSA)	29
2.6. Immunoprecipitation and identification of glutathionylated proteins	30
2.7. Modified Biotin Switch assay	30
2.8. Apoptosis hallmarks identification by flow cytometry	31
2.9. Immunofluorescence and confocal analysis	31
2.10. Measurement of intracellular reactive oxygen species	32
2.11. Measurement of nitrite and nitrate	32
2.12. Cross-talk <i>in vitro</i> cellular model	33
2.13. Statistical analysis	34
3. Results	35
3.1. Oxidative stress induces the S-glutathionylation of STAT1 and activates its signaling cascade in BV2 cells	35

3.1.1.	Oxidative stress induces phosphorylation of STAT1 in BV2 cells	35
3.1.2.	Oxidative stress induces S-glutathionylation of STAT1 in BV2 cells	36
3.1.3.	Cys324 and Cys492 are targets of S-glutathionylation of STAT1 in BV2 cells	37
3.1.4.	Oxidative stress induces apoptosis in BV2 cells	39
3.2.	M1 microglia activation under hypoxia: the key role of STAT1	41
3.2.1.	Hypoxia induces phosphorylation of STAT1 in BV2 cells	41
3.2.2.	Hypoxia induces S-glutathionylation of STAT1 in BV2 cells	43
3.2.3.	Hypoxia triggers the transition to M1 phenotype in BV2 cells	44
3.2.4.	Hypoxia leads to M1 phenotype activation through the activation of STAT1 signaling in BV2 cells	47
3.2.5.	Hypoxia activated BV2 cells induce SH-SY5Y cells apoptosis	49
3.3.	Myricetin counteracts M1 activation of BV2 cells induced by hypoxia	52
3.3.1.	Myricetin counteracts M1 phenotype activation induced by hypoxia in BV2 cells	52
3.3.2.	Myricetin counteracts STAT1 phosphorylation induced by hypoxia in BV2 cells	55
3.3.3.	Myricetin prevents SH-SY5Y death induced by hypoxia-activated BV2 cells	57
4.	Discussion and conclusion	59
5.	Bibliography	63
6.	Appendix	76

1. Introduction

1.1. Signal Transducer and Activator of Transcription 1

Signal Transducer and Activator of Transcription 1 (STAT1) is a member of a family of seven transcriptional factors (STAT1, 2, 3, 4, 5a, 5b and 6) that mediate the regulation of transcription of genes involved in several biological events such as embryonal development, organogenesis, innate and adaptive immunity, cells growth and differentiation, and programmed cell death [1], [2]. In resting cells, STATs proteins are latent in cytoplasm and they translocate to the nucleus after specific stimuli. The classical activation pathway involves the binding of cytokines or growth factors to a specific receptor on cell surface. The STATs activation mechanism requires the phosphorylation on conserved tyrosine and serine residues by Janus tyrosine kinases (JAKs) and Mitogen-Activated Protein Kinases (MAPKs), respectively. This event allows the dimerization of phosphorylated STATs and their translocation into the nucleus where they modulate the expression of target genes [3], [4].

Specifically, STAT1 is the key effector of type I and II interferons (IFNs) but it is activated also by other cytokines (e.g. interleukins IL-2, IL-6) and growth factors (e.g. Factor Epidermal growth factor, EGF, or Platelet Derived Growth Factor, PDGF) [5]. This signaling pathway controls the whole inflammatory process regulating the expression of several proteins such as the Inducible Nitric Oxide Synthase (iNOS), the Cyclooxygenase 2 (COX2), the Vascular Cellular Adhesion Molecule (VCAM) and the Intercellular Adhesion Molecule (ICAM) [6]. Moreover, STAT1 induces the transcription of several genes involved in the regulation of cell proliferation. In particular, its activation determines a pro-apoptotic effect inducing caspases expression and NF- κ B inhibition [7]. STAT1 promotes the apoptotic process in response to the inflammatory stimulus (e.g. cytokines) but also to other stimuli like ischemia, heat and DNA damage. During the last decade, it has been described the key role of STAT1 in non-apoptotic cell death through the necrotic or autophagic processes [8]. In both these mechanisms, the STAT1 signaling activation is due to a deregulation of Reactive Oxygen Species (ROS) [9]–[11]. STAT1 activation is strictly regulated spatially and temporally during the inflammatory response; the deregulation

of this pathway can lead to massive cells or tissue damage. A persistent or excessive STAT1 activation has been observed in many diseases correlated to acute or chronic inflammation such as ischemic/reperfusion damage, asthma, coeliac disease, atherosclerosis, psoriasis and rheumatoid arthritis [9], [12], [13]. Furthermore, the subjects carrying a mutation on STAT1 protein expression are more susceptible to bacterial and viral infections [14], [15].

1.1.1. STAT1 Structure

STAT1 is a protein composed of 750 amino acids that weights about 91KDa (STAT1 α). The 3D-structure of STAT1 protein has been determined thanks to two crystals deposited on the Protein Data Bank (PDB): the unphosphorylated form 1YVL and the Tyr701-phosphorylated one 1BF5 (Fig.1) [16].

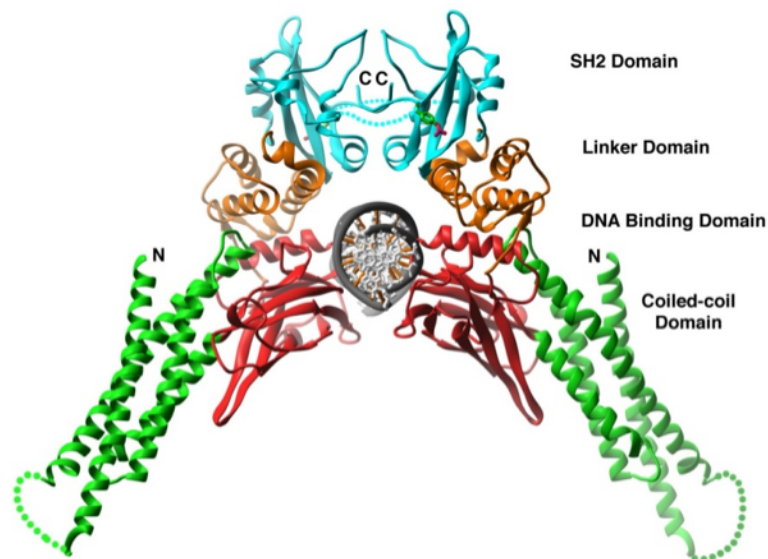


Figure 1. 3D structure of STAT1 dimer binding the DNA double helix (PDB: 1BF5).

Likewise the other STAT family members, STAT1 protein is constituted by six functional domains (Fig.2) [17]:

- N-terminal domain (NTD), aa 1-134, involved in the active dimer formation, in the interaction with transcription co-activators, in the regulation of nuclear translocation and in cooperative binding to DNA.

- Coiled-Coil Domain (CCD), aa 135-317, linked to the NTD through a flexible polypeptide chain. It is a four- α -helical domain which constitutes a hydrophilic surface that allows the interaction with regulatory proteins. The CCD participates also in other events such as the binding with the receptor, the Tyrosine phosphorylation and the nuclear export.
- The DNA Binding Domain (DBD), aa 318-488, is constituted by a β -barrel folded in an immunoglobulin-like structure. The DBD binds a specific DNA sequence, called Gamma-interferon Activated Site (GAS).
- The Linker Domain (LD), aa 489-576, that links the DBD and the following SH2 domain and it is involved in the regulation of transcription. Some evidence show that the LD is necessary for nucleocytoplasmic cycling because the alkylation of a single cysteine residue impair the nuclear translocation of STAT1 [18].
- The tyrosine-binding Src Homology 2 Domain (SH2D), aa 577-683, is the most conserved among STAT family due to its key role in receptor recruitment, phosphorylation and dimerization. The SH2D consists in an antiparallel β -sheet with two α -helices alongside forming a pocket containing the Arg602 residue, highly conserved, that mediate the interaction with the phosphate group. These structural features make the SH2D able to recognize the phosphor-tyrosine residues on specific protein regions determining the association with the activated JAKs and the subsequent dimerization of STAT. The variations in SH2 domains determine the selective receptor binding on each STAT. It has been reported that mutations within this domain affect the DNA binding ability and the consequent gene transcription efficiency after IFN- γ stimulation [19].
- The C-terminal Transcriptional Activation Domain (TAD), aa 684-750, regulates the transcriptional specific response and it is the less conserved domain. The key event for STAT1 activation, dimerization, import in the nucleus and DNA binding is the Tyr701 phosphorylation located within a region called "Tyrosine Activation Motif" present on a flexible loop between the SH2D and the TAD. Also the Ser727 residue is a phosphorylation site important for the regulation of STAT1 transcriptional activity and for the recruitment of co-activators. In fact, it has been reported that the

phosphorylation of Ser727 is crucial to obtain the maximum transcriptional efficiency since the activity is reduced by 20% when STAT1 protein is mutated at Ser727 [20]. The kinases responsible for this event belong from the MAPK family such as the Extracellular signal Regulated Kinases (ERK), the c-jun N-terminal kinase (JNK) and the p38 [21].

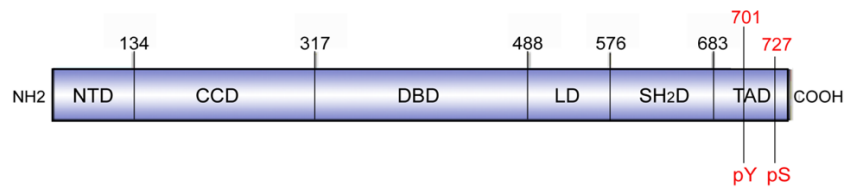


Figure 2. Schematic structure of functional domains and protein phosphorylation sites of STAT1 protein. Scheme of functional domains of STAT1: N-terminal domain (NTD), Coiled-Coil domain (CCD), “DNA Binding” domain (DBD), linker domain (LD), SH2 domain (SH2D) and transcriptional activation domain (TAD). The phosphorylation sites are highlighted in red: Tyr701 and Ser727.

Several splice-variants of STATs proteins have been identified so far. This β isoforms, lacking of C-terminal portion, are still involved in the gene transcriptional process interacting with other transcriptional factors. In particular, they act as dominant-negative binding the same target gene promoters on DNA and blocking STATs-mediated gene transcription [22]. The alternative splicing of STAT1 mRNA determines the expression of the STAT1 β isoform which is lacking of the TAD domain, essential for the transcriptional activity of STAT1, and transcriptionally inactive [23]. STAT1 β , truncated at the C-terminal, conserves the phosphorylation site on Tyr701 residue and it can compete with the full-length isoform, STAT1 α , for the binding to the DNA [24], [25]. Recently, the biological activity of STAT1 β has been re-evaluated since new data suggest that this truncated isoform can promote cellular death through a different mechanism from those induced by STAT1 [26].

1.1.2. STAT1 signaling pathway

The classical pathway of signal transduction mediated by STATs factors is activated through phosphorylation events triggered by the formation of the receptor complex between a cytokine or a growth factor exposed on the cellular membrane (Fig.3). In particular, the STAT1 is activated by the binding of cytokines, such as type I and II

IFN, IL-6, IL-11 and AT-1, or growth factors, like EGF, PDGF, CSF-1 and HGF, to the specific receptor on cell surface [27], [28]. Following the interaction between cytokine and receptor, specific JAKs kinases (JAK1, JAK2 and Tyk2), associated to intracellular domains of the receptor, are activated through auto- and trans-phosphorylation. This event leads to the phosphorylation of other tyrosine residues present on the receptor itself and, consequently, to the recruitment of the STAT factors. The cytoplasmic latent monomeric STAT1 protein thus associated with the receptor is phosphorylated at tyrosine 701 by JAKs kinases [29], [30]. The phosphorylated STAT1 monomers constitutes homo- or hetero-dimers (with other STATs proteins e.g. STAT2) through the reciprocal interaction between the SH2 domains. Then, the STAT1 dimers can migrate and accumulate into the nucleus where they regulate the gene transcription. The maximum transcriptional activity of STAT1 is obtained with the phosphorylation of the Ser727 residue, presented in a conserved sequence within the STATs family in the C-terminal domain [20].

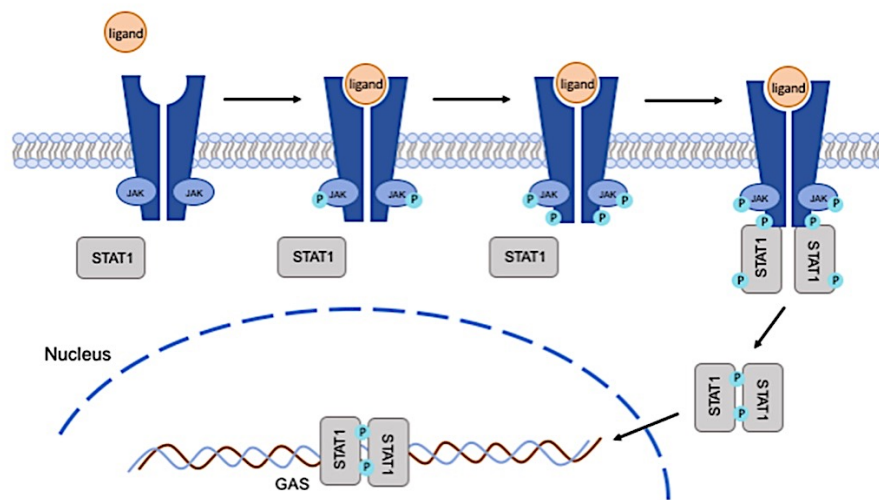


Figure 3. JAK/STAT1 pathway. STAT1 is activated by the binding of cytokines growth factors to the specific receptor on cell surface. JAKs kinases, associated to the receptor, are activated through phosphorylation leading to the phosphorylation of the receptor itself. The cytoplasmic STAT1 protein associates with the receptor and it is phosphorylated. STAT1 dimers can migrate and accumulate into the nucleus where they regulate the gene transcription binding a specific GAS sequence on DNA.

The transcriptional response of STAT1 to cytokine signal is transient: the STAT1 accumulation into the nucleus requires minutes after stimulation with IFN and the its

export occurs within hours [31]. Generally, the molecular trafficking between the cytoplasmic and nuclear compartments occurs through membrane structures called Nuclear Pore Complexes (NPC), barrel-shaped complexes constituted by nucleoporins (Nups). The small molecules (<40-60 kDa) can get across the NPC through passive diffusion, the larger molecules (>60 kDa), instead, like the STATs proteins, requires facilitated transport mediated by transport proteins that recognized specific signal sequences [32]–[34]. STAT1, like all STATs proteins, includes a Nuclear Localization Signal (NLS) sequence, rich in basic amino acids (e.g. lysine and arginine), identified by specific nuclear receptors, called α 5- and β -importins. These receptors recognized a specific NLS sequence within the DBD and exposed only by the STAT1 active, dimeric and Tyr701-phosphorylated conformation. Also the Leu407 residue and the NTD are important for the correct NLS conformation [35], [36]. The importin-STAT1 complex interacts with the NPCs on the cytoplasmic side of the nuclear membrane and it moves into the nucleus where the complex dissociates enabling the binding between STAT1 and the target sequence of the DNA [37]. It has been reported that also the unphosphorylated dimer of STAT1 can move into the nucleus but through which mechanism is still unclear. It seems that, unlike dimeric phosphorylated STAT1 that needs the facilitated transport, the unphosphorylated dimer does not require the intervention of other cytoplasmic proteins to interact with NPC [35]. The metabolic energy requested for the active nuclear trafficking comes from a protein member of G proteins family, called Ran [38]. Regarding the nuclear export process, instead, the STATs proteins present hydrophobic regions, rich in leucine residues, called Nuclear Export Signal (NES), recognized by specific transporter proteins, called exportins [39]. The Chromosome Region Maintenance 1 (Crm1) is one of the main exportins involved in STAT1 nuclear export. In the nucleus, Crm1 identifies the specific NES sequence, within the DBD, and recruits a Ran-GTP forming a ternary complex. The NES sequence is hidden as long as STAT1 is associated to the DNA and becomes reachable only once STAT1 is dephosphorylated (Fig.4) [40].

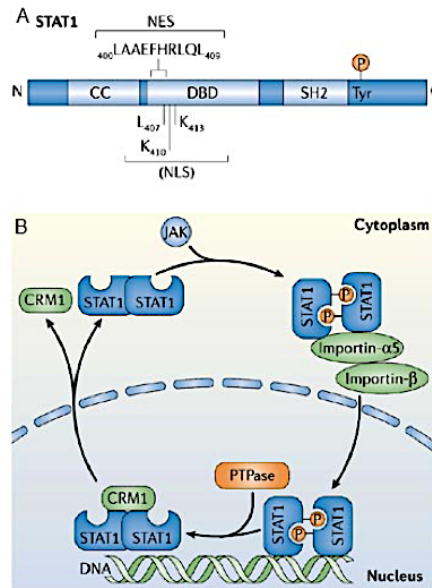


Figure 4. Nuclear import-export regulation of STAT1. Regolazione dell'import-export nucleare di STAT1. A) NLS sequence within STAT1 structure. B) Mechanism of nuclear import-export of STAT1. doi.org/10.1038/nri1885.

The intensity and the duration of JAK/STAT signaling is regulated also by the intervention of regulatory proteins that inhibits the transduction pathway through different mechanisms mainly promoting the dephosphorylation of the JAKs and the STATs and their export from the nucleus. The protein families involved in the negative regulation of the pathway are the Protein Tyrosine Phosphatases (PTP), the Suppressors Of Cytokine Signaling (SOCS) and the Protein Inhibitors of Activated STATs (PIAS) (Fig.5) [41].

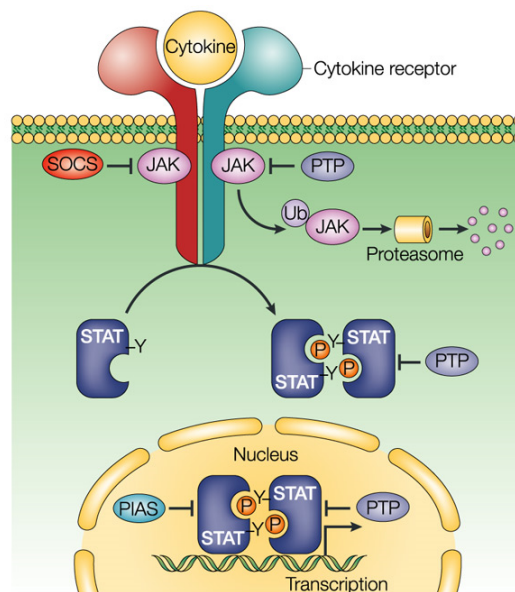


Figure 5. Negative regulation of JAK/STAT pathway. PTP phosphatases are involved in dephosphorylation of both JAKs and STATs. SOCS proteins, induced by cytokines, switch off the JAKs acting as a negative-feedback loop. PIAS proteins interact with STATs in the nucleus after cytokine stimulation and inhibit their transcriptional activity. doi:10.1038/nri1226

The PTP are a phosphatases family involved in the dephosphorylation of JAKs and STATs proteins. In particular, within the PTP family, the SH2-phosphatases (SHP) are characterized by a SH2 domain that recognizes the phosphor-tyrosine residues. Among them, the cytoplasmic SHP1, mainly expressed in the hematopoietic tissue, is responsible for JAK1 and JAK2 inactivation, and SHP2, ubiquitous and present both in cytoplasm and in nucleus, dephosphorylates JAK1. SHP2 directly inactivate STAT1 dephosphorylating both p-Tyr701 and p-Ser727 residues [42]. Other PTP involved in the inhibition of STAT1 signaling are PTP1B, a specific inhibitor of JAK2 and TYK2 and T-Cell PTP (TCPTP) that act on JAK1. The nuclear isoform of TCPTP, called TC45, dephosphorylates p-Tyr701-STAT1 impairing its transcriptional activity and inducing its export from the nucleus [43].

The SOCS family includes eight intracellular proteins that have a key role in protein degradation process through the ubiquitin/proteasome pathway. SOCS proteins, such as SOCS1 and SOCS3, are characterized by the presence of a central SH2 domain and by a conserved region, called SOCS BOX, that directly binds the ubiquitin E3 ligase complex leading to kinases degradation [44]. The SOCS expression is quickly induced

by the same cytokines that trigger the JAK/STAT pathway causing the inhibition of STATs signaling through a negative feed-back mechanism [45]. Among the SOCS family, SOCS3 inhibits the activated complex of the cytokine receptor while SOCS1 interacts directly with the phosphorylated JAKs [44]. Another member of the same protein family, the Cytokine-Induced SH2 domain protein (CIS), competes with STAT for the binding to the cytokine receptor, counteracting the signaling activation [46].

The nuclear regulators family, called also PIAS, consists in four proteins (PIAS1, PIAS3, PIASX and PIASY) that interact with STATs activated dimers preventing their association with DNA and the gene transcription [47]. The specific PIAS-STAT interaction is cytokine-dependent and within the PIAS family the different proteins act through different mechanisms. Only PIAS1 and PIASY are involved in the regulation of STAT1 pathway. PIAS1 directly associates with the promoters of STAT1 target genes blocking the transcriptional process mediated by this factor [48]. PIASY, instead, does not influence the ability of STAT1 of binding DNA and is considered a co-repressor of STAT1 activity by recruiting of Histone Deacetylase (HDAC) and other co-repressor proteins [49]. PIAS proteins have been shown to act also through a SUMO E3 ligase-like mechanism; in fact, they promote the conjugation of transcriptional factors with the Small Ubiquitin-like Modifier (SUMO); SUMO is a small protein, that, despite being similar to ubiquitin, is not a degradation tag but is involved in a regulatory post-translational modification. It has been shown that STAT1 is SUMOylated on Lys703 after IFN γ stimulation and that it is enhanced by PIAS1 but whether this modification effectively has a role in the regulation of STAT1 activity is still unclear [50].

Besides the classical pathway of STAT1 activation, whereby it dimerizes after Tyrosine phosphorylation, it has been reported that also a cytoplasmic non-phosphorylated dimer of STAT1 can enter in the nucleus, bind the DNA and promote the transcription of genes related to cellular resistance to genotoxic stress [51], [52]. In this regard, two different theoretical models were proposed: the dimer phosphorylated at Tyr701, oriented parallel, and a non-phosphorylated one with antiparallel orientation. The parallel conformation model is characterized by the interaction between the SH2 domain of a monomer and the phosphor-tyrosine of the other one; in the antiparallel model, instead, the SH2 domains of the two monomers involved are oppositely

oriented and the dimer formation is due to NTD-NTD and CCD-DBD interactions (Fig.6) [53].

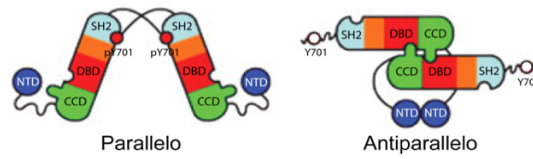


Figure 6. Conformational models of STAT1 dimers. doi/10.1101/gad.1485406.

1.1.3. Regulatory post-translational modifications of STAT1

Aside from the phosphorylation and SUMOylation, STAT's activity can be regulated by other post-translational modifications, such as ubiquitylation, acetylation, methylation and ISGylation. It has been reported that STAT1 can undergoes ubiquitylation and degradation through ubiquitin-proteasome pathway [54]. Also acetylation has a role in negative regulation of STAT1 activity. Histone acetyltransferase CBP induces the acetylation of Lys410 and Lys413 residues of STAT1 leading to the dissociation of the DBD from the promoter sequences and the protein dephosphorylation by protein phosphatase PTPN2 [55]. The methylation and ISGylation, instead, have a positive regulatory role in STAT1 signaling pathway. The STAT1 methylation on Arg31 is mediated by Protein Methyl-Transferase 1 (PRMT1), an enzyme associated also with the IFN α/β receptor. This event seems to be constitutive, independently of tyrosine/serine phosphorylation, and it increases the STAT1 ability to bind DNA inhibiting the interaction with PIAS1 [56]–[58]. Interferon-Stimulated Genes (ISG) proteins have been reported to regulate JAK/STAT1 pathway by conjugating both JAK1 and STAT1 and acting within a positive feed-back loop [59].

1.2. Oxidative stress and S-Glutathionylation

1.2.1. Cellular redox state and ROS homeostasis

Aerobic organisms are characterized by a fine balance between the production of oxidant molecules, such as the Reactive Oxygen Species (ROS) and the Reactive Nitrogen Species (RNS), and the antioxidant cellular systems. The ROS and RNS include radical and non-radical species produced through the partial reduction of oxygen or nitrogen during mitochondrial oxidative metabolism or in cellular response to exogenous cytokines, xenobiotics, and pathogens invasion [60]. Under physiological condition, low and controlled amounts of ROS or RNS have a role as second messengers in intracellular signaling pathways. It has been demonstrated that ROS directly interact with signaling molecules involved in several cellular processes, such as, proliferation and survival (e.g. MAPK, PI3K, PTP), ROS homeostasis and antioxidant genes regulation (thioredoxin, peroxiredoxin, Ref-1, and Nrf-2) and apoptosis (e.g. Bax, Bid, Myc) [61]. However, when the amount of ROS/RNS within the cells overwhelm the antioxidant defense system, whether through an excess of oxidant species levels or a deficiency in antioxidant capacity, oxidative stress occurs [62]. Oxidative stress results in direct or indirect damage to macromolecules (e.g. nucleic acids, proteins, lipids) and it has been implicated in different diseases such as atherosclerosis, ischemia-reperfusion damage, cancer, neurodegeneration, diabetes, asthma and aging [63]–[67].

Under physiological condition, several enzymatic and non-enzymatic antioxidant mechanisms protect the cells from oxidative damage maintaining the intracellular environment in a reduced state. The enzymatic defense against oxidative stress involves proteins, like the superoxide dismutase (SOD), the catalase, the glutathione peroxidase (GPxs), the glutathione transferase (GST) and the glutathione reductase (GR). The antioxidant non-enzymatic systems include molecules that act as ROS scavengers like α -tocopherol (vitamin E), β -carotene (precursor of vitamin A) and the ascorbic acid (vitamin C) [68]. The most important ROS scavenger is the thiols pool, consisting of low molecular weight compounds like glutathione (GSH) and of proteins amino acidic residues like cysteine and methionine [69]. Furthermore, multiple and

interrelated redox couples, such as the reduced/oxidized nicotinamide adenine dinucleotide phosphate NADPH/NADP⁺, the reduced/oxidized glutathione GSH/GSSG, the reduced/oxidized thioredoxin Trx/TrxSS, and cysteine/cystine, contribute to the maintenance of intracellular redox homeostasis [69]–[71].

1.2.2. The glutathione and the redox couple GSH/GSSG

The glutathione, (GSH) is a ubiquitous hydrophilic tripeptide constituted by three amino acids: γ -glutamic acid, cysteine and glycine. The GSH biosynthesis occurs in cytoplasm through a two steps mechanism. The first and rate-limiting step is the formation of γ -glutamine-cysteine starting from L-glutamate and cysteine, catalyzed by the glutamate-cysteine ligase (GCL). The second step is a reaction of condensation between the C-terminal of γ -glutamine-cysteine and glycine, catalyzed by the glutathione synthetase [72]. Following its biosynthesis, GSH is present within all mammalian cells with a concentration ranging from 1 to 10mM, depending on the cellular compartment considered [73], [74]. It is mainly located in cytosol (90%) whereas only a little amount is present in other cellular compartments such as mitochondria endoplasmic reticulum and nucleus [75]. Intracellular glutathione can exist as a monomer in its reduced form (GSH) or as a disulfide dimer (GSSG) after its oxidation which usually accounts for less than 1% of the total intracellular glutathione content. In physiological conditions, the GSH/GSSG is the main redox couple in living cells and the proper ratio between the levels of GSH and GSSG, is essential in maintaining the homeostasis of intracellular redox state (Fig.7) [69], [76].

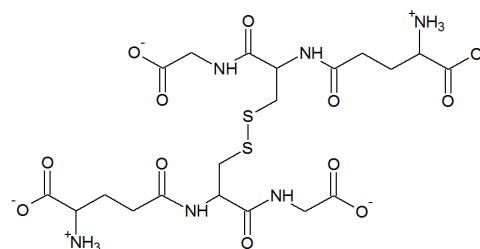
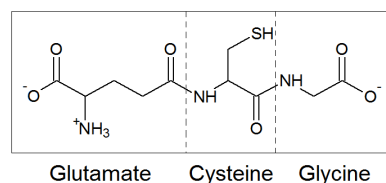


Figure 7. Glutathione and glutathione disulfide dimer structures.

As antioxidant agent, GSH can act both as direct scavenger of free radicals and as substrate of glutathione-dependent enzymes, such as GR, GPxs and GST (Fig.8) [77].

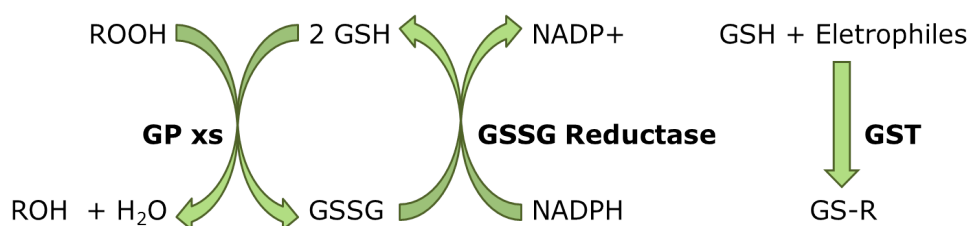


Figure 8. Scheme of antioxidant glutathione-dependent enzymes reactions. The major glutathione-dependent enzymes of the antioxidant system in cells are GPxs, GSSG Reductase and GST. GPx is a peroxidase that reduces peroxides using GSH as cofactor. GR or GSSG reductase catalyzes the reduction of GSSG to GSH. GR requires NADPH to reduce one molar equivalent of GSSG to two molar equivalents of GSH. GST catalyzes the conjugation of GSH to xenobiotic substrates.

The intracellular redox state is provided by a high GSH/GSSG ratio, since about 98% of the cytoplasmic glutathione is in the reduced form. When oxidative stress occurs, the equilibrium of this ratio shifts toward the oxidized form determining the partial or complete reversible oxidation of free thiols groups exposed by proteins. When the GSH/GSSG ratio is slightly unbalanced, the redox homeostasis is preserved by regulating the GR enzyme activity which reduces the GSSG to GSH, or improving the GSSG transport outside the cell [78]. Nevertheless, in presence of excessive oxidative

stress, these mechanisms are not enough to preserve the proper redox balance and the irreversible macromolecules oxidation may occur resulting in cellular death [79].

1.2.3. Protein cysteinyl thiols and S-Glutathionylation

As previously described, oxidative stress determines reversible and irreversible oxidation of specific thiol groups on proteins impacting their structure and function [80]. The main factors required to make a cysteine susceptible to redox reactions are the accessibility in the 3D structure of the protein and the reactivity of thiol groups that is influenced by neighboring amino acids. Most of the thiol groups of cysteine residues within proteins in the cytoplasm are characterized by a pK_a value > 8 ; therefore, they are protonated at physiological pH and, in the reducing intracellular environment, they are not sensitive to oxidation. However, some redox-sensitive cysteine residues are located in a basic environment (neighboring amino acids like histidine, arginine or lysine) or form hydrogen bonds with the nearby hydroxyl groups (serine or tyrosine residues). This environment lowers the pK_a value and allows the formation of the thiolate anion, deprotonated and susceptible to oxidative modifications [81], [82].

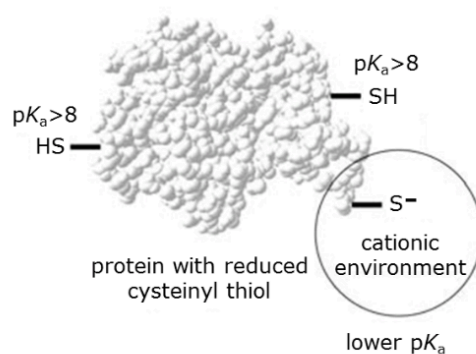


Figure 9. Redox-sensitive cysteines position within the 3D structure of a protein. Redox-sensitive cysteine residues are located in a basic environment or form hydrogen bonds with the nearby hydroxyl groups. This environment lowers the pK_a of thiol group to a less than 8 value allowing its deprotonation and the formation of the thiolate anion, susceptible to oxidative modifications.

Under oxidative stress, redox-sensitive thiol groups of proteins (**P-SH**) can be oxidized to form:

- sulfenic acid (**P-SOH**), through a reaction with H_2O_2 or other peroxides. This is an unstable compound that promotes further oxidation steps.
- sulfinic (**P-SO₂H**) or sulfonic (**P-SO₃H**) acids. These modifications are irreversible and leads to the protein misfolding or to the formation of aggregates.
- intramolecular (**P-SS-P**) or intermolecular (**P-SS-X**) disulfide. Specifically, when this latter reaction occurs with glutathione, the derived post-translational modification is known as S-glutathionylation (GSS-P) [81].

All these modifications can potentially affect folding and protein activity, depending on the importance of the cysteine residue in carrying out protein function [83].

S-glutathionylation, the formation of a mixed disulfide between glutathione and redox sensitive protein sulfhydryl groups, is a reversible post-translational modification that may protect proteins from irreversible damage or modulate protein functions [84], [85]. The reversibility of this post translational modification is guaranteed by the intervention of Trx and Grx enzymatic systems [86]. Besides the redox regulation function, the S-glutathionylation can occur in some proteins also in basal conditions suggesting that this modification could be involved in physiological cellular signaling [77], [87].

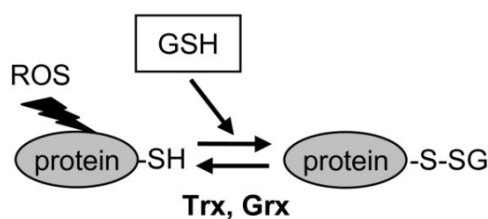


Figure 9. Scheme of S-glutathionylation mechanism. The reaction of S-glutathionylation consist in the formation of a mixed disulfide between glutathione and redox sensitive sulfhydryl groups of proteins. It is a reversible post-translational modification that protect proteins from irreversible oxidation or modulate protein functions. The reversibility of this post translational modification is guaranteed by the intervention of Trx and Grx enzymatic systems. doi: 10.1186/1471-2091-11-3.

Despite the fact that the molecular mechanism of the S-glutathionylation reaction has not been clarified, several possibilities have been proposed as response to GSH/GSSG ratio changes (Table 1) [88].

$P-SH + GSSG \rightarrow P-S-SG + GSH$	Thiol/disulphide exchange reactions between protein sulphhydryl group and GSSG.
$P-S^{\bullet} + GS^{-} + O_2 \rightarrow P-S-SG + O_2^{\bullet-}$	Reaction between the thyl radical, obtained from the partial oxidation of the protein thiol group and the GS^{-} .
$P-S^{-} + GS^{\bullet} + O_2 \rightarrow P-S-SG + O_2^{\bullet-}$	Reaction between the thyl radical and the thiolate group of the protein.
$P-SOH + GSH \rightarrow P-S-SG + H_2O$	Reaction between the sulphhydryl group of the protein, oxidized to sulfenic acid, and GSH.
$P-SNO + GSH \rightarrow P-S-SG + HNO$	Reaction between the S-nitrosated sulphhydryl group of the protein and GSH.
$P-SH + GSNO \rightarrow P-S-SG + HNO$	Reaction between the S-nitrosated sulphhydryl group of GSH and the thiol group of the protein.
$P-SH + GSOH \rightarrow P-S-SG + H_2O$	Reaction between the GSH, oxidized to sulfenic acid, and the thiol group of the protein.

Table 1. Proposed mechanism for S-glutathionylation.

In the last ten years, numerous research groups became interested in the S-glutathionylation because it represents a new post-translational modification mechanism and it has been found to be important in several disease etiology [87], [89], [90]. Most of S-glutathionylated proteins are enzymes involved in energetic metabolism, are part of the cytoskeleton or are involved in transcription and transduction processes [87]–[89].

1.3. Neuroinflammation

Neuroinflammation is a pathophysiological condition closely related to the onset and the progression of most neurodegenerative diseases such as Alzheimer's disease, Parkinson's disease, amyotrophic lateral sclerosis and Huntington's disease [94], [95]. Today, in the degenerating Central Nervous System (CNS), the role of inflammation is seen as double-edged sword by scientists since it might either accentuate or inhibit the neurodegenerative process [96]. Inflammation is a defensive reaction played by multicellular organisms against various insults aimed at removing the noxious agents and protecting tissues from their damaging effects. In neurodegenerative diseases, inflammation may be triggered by pathogenic insults, abnormal protein aggregates, signal molecules released by damaged glia or neurons, or by the imbalance of pro-inflammatory and anti-inflammatory factors [97]–[101]. In general, the different outcomes of inflammation could be: the insulting agent is inhibited and the injury repaired, the host organism is overpowered because of the excessive damage on tissue, or neither of the two prevails promoting the establishment of a chronic inflammatory condition. This latter outcome is considered closely related to neurodegenerative diseases [102]. At first, the inflammatory reactions engages the innate components of CNS immune system; then, in a second phase, also the acquired immune response is involved [96]. In fact, microglia and astrocytes, the major effectors of CNS innate immune system, are strongly activated in most neurodegenerative diseases [103]–[105]. Despite being pathological mediators, the resting and activated astrocytes and microglia have an important physiological role in development, plasticity and repair of CNS, as well as in maintaining homeostasis [106]–[109]. However, these glial species are both source and target of proinflammatory mediators and reactive oxidants at the injured site; for this reason, they might have potentially detrimental effects on neuronal cells, following an aberrant or prolonged activation [110].

1.3.1. Microglia activation

Microglia are the resident mononuclear phagocyte cells in the CNS where they are involved in important processes such as innate immune response, antigen presentation, phagocytosis, CNS tissue development maintenance of neural environment and stem cells proliferation [111]. In particular, due to its key role in

mediating the inflammatory process, microglial cells activation is considered the hallmark of neuroinflammation. Pro-inflammatory factors (e.g. lipopolysaccharide), environmental toxins (rotenone, paraquat, particular matter), may endogenous disease proteins (e.g. β -amyloid peptide, α -synuclein) may lead to microglia activation [112]–[116]. Moreover, microglia is activated also in response to neuronal damage. In fact, injured or dying neurons can activate microglia that, in turn, produce neurotoxic factors (e.g. pro-inflammatory cytokines and reactive oxidative species), giving rise to a self-propelling vicious cycle of neuronal death. This process is called reactive microgliosis and could participate in the progression of several neurodegenerative disease [101].

Like other tissue-specific resident macrophages, microglia constitute about the 10% of cell population in brain tissue. Under basal condition, microglia assume a “resting” quiescent phenotype, characterized by a ramified morphology, that constantly scan the brain parenchyma thanks to the high mobile and dynamic processes and protrusions [117]. This surveilling state is promoted, in part, by neuron-derived factors (e.g. CX3CL1, CD22, CD47, CD200) recognized by receptors expressed on the plasma membrane of microglial cells. Moreover, microglia membrane presents also a variety of toll-like receptors (TLRs) that allow the recognition of a large number of exogenous agents. The random monitoring by processes can eventually and rapidly evolve in a targeted movement towards an injured site, switching to an activate functional phenotype [118]. Upon exposure to pro-inflammatory cytokines, IFN γ , Tumor Necrosis Factor α (TNF α), bacterial-derived products (LPS), or cellular debris, microglia assume the classical pro-inflammatory activated phenotype (M1), characterized by hypertrophic bodies and amoeboid shape with fewer, shorter and thicker processes than those of resting microglia [119], [120]. A similar response can be triggered by trauma, chemical exposure or ischemic/reperfusion injury [114], [121]–[123]. After activation, M1 microglia produce pro-inflammatory factors (like TNF α , Interleukin (IL)-12, IL-1 β , IL-6, chemokines), present antigens through MHCII factors and express redox factors such as NADPH oxidase (NOX) and inducible Nitric Oxide Synthase (iNOS) [117], [124]–[126]. The activation of NOX and iNOS lead to the release of ROS and RNS that rapidly reinforce the inflammatory response. Microglia-dependent neuroinflammatory process involves multiple signaling cascades,

including Nrf2, NF- κ B and STAT1 which plays a key role in the regulation of inflammatory response as well as cellular death [127], [128]. It has been described that STAT1 is activated in several neurodegenerative diseases associated with neuroinflammation. For example, STAT1 activation induces β -secretase 1 (BACE1) expression and amyloid beta production in astrocytes and neurons, activates transcription of pro-inflammatory genes, such as COX-2 and iNOS, in microglia cells in Alzheimer's disease context [129]–[131].

During the '90s, the idea of macrophage alternative activation was developed, mainly based on the capacity of IL-4 in inducing a cytoprotective phenotype called alternative or M2 phenotype [132]. Anyway, it has been reported that human microglia has a reduced capability to establish this M2 phenotype compared to the blood derived macrophages [133]. Thus, the pro-inflammatory M1 polarization of microglia can be followed by an extended repair phase where M2 microglia is activated. M2 phenotype cells present thin bodies, thick branched processes [125], [134]. Similar to macrophages, the M2 transition is triggered by anti-inflammatory cytokines like IL-4, IL-13 and IL-10, glucocorticoids, immunoglobulin complexes/TLR) and Transforming Growth Factor β (TGF β). Upon activation, M2 microglia present low levels of pro-inflammatory factors but release IL-4, IL-5, IL-10 and IL-13 and express several healing genes (e.g. nerve and insulin growth factors, scavenger receptors, CD36, CD163, PPAR- γ , arginase-1, FIZZ1) [135]. The signaling cascades involved in M2 microglia are still not completely clear but IL-4-dependent signaling through STAT3 and STAT6 pathways seems to be important [136], [137]. Consequently, M2 phenotype activation of microglia has a key role in switching-off the inflammatory process, restoration of the damaged extracellular matrix and scavenger cellular debris [138]. The M2 polarized state can be subdivided into M2a, M2b and M2c subtypes depending on the mechanism of activation and the function [139].

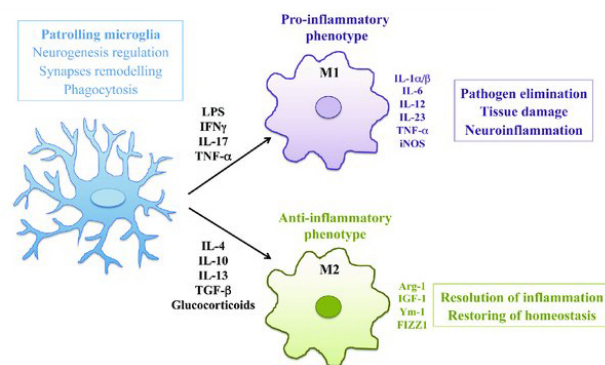


Figure 10. Scheme of microglia activated phenotypes. In physiological conditions “resting” microglia regulate CNS homeostasis. In neuroinflammation microglia acquire classical M1 or alternative M2 phenotype depending on the detected stimulus. doi: 10.3389/fnagi.2017.00148.

However, this classification of microglia into “resting” or M1 and M2 polarized phenotypes is considered an oversimplification. In fact, microglia cells are characterized by high plasticity and diversity and these states described above represent more an array of activation models rather than actual separate subtypes [139].

Therefore, microglia are crucial to maintain the CNS homeostasis but an uncontrolled activation can lead to neuron damage. In particular, chronic activated microglia, sustained also by activated astrocytes, release a variety of pro-inflammatory and cytotoxic factors, such as ROS, leading to a self-sustaining inflammatory cycle with neurotoxic outcomes [98], [140], [141].

The microglia activation towards M1 phenotype is strictly correlated to the redox environment. ROS/RNS levels are normally low in “resting” microglia but they increase extremely during M1 transition due to the activation of NOX and iNOS enzymes [132]. These reactive species act also on surrounding cells but the main target are microglial cells themselves, because of the proximity of the production site and high reactivity. Therefore, ROS/RNS represent the driving force in pathological microglia over-activation.

ROS/RNS were generally considered as cytotoxic species, but recently their ability of to induce post-translational modifications on redox-sensitive proteins in physio-pathological context has been described [89]. For example, it has been demonstrated

the role of protein S-gluthionylation in monocyte and macrophage dysfunction as a link between oxidative stress and metabolic disorders or chronic inflammatory diseases [142]. Nitrosylation mediates the inhibition of the insulin-degrading enzyme occurs in presence of oxidative stress in murine microglia BV2 cells, causing the impairment of A β peptide degradation and contributing to Alzheimer's disease progression [143]. In the same way, α -synuclein, the main constituent of Lewi bodies Parkinson's disease, is nitrated because of the oxidative stress triggering the inflammatory process in microglial cells [144].

2. Materials and methods

2.1. Reagents

All chemicals used throughout the present study were of the highest analytical grade, purchased from Sigma, unless otherwise specified. Dulbecco's modified Eagle's medium (DMEM), Roswell Park Memorial Institute Medium (RPMI) and fetal bovine serum (FBS) were obtained from Thermo Fisher Scientific.

2.2. Cell cultures

Murine microglial BV2 cells were cultured in RPMI supplemented with 10% FBS, 100UI/mL penicillin, 100µg/mL streptomycin and 40µg/mL gentamycin in a 5% CO₂ atmosphere at 37°C. Human neuroblast-like SH-SY5Y cells were cultured in DMEM supplemented with 15% FBS, 1% Non-Essentials Amino Acids, 100UI/mL penicillin, 100µg/mL streptomycin and 40µg/mL gentamycin in a 5% CO₂ atmosphere at 37°C. Hypoxic culture conditions were achieved with a multi-gas incubator containing a gas mixture composed of 94% N₂, 5% CO₂, and 1% O₂ (RUSKINN C300, RUSKINN Technology Ltd) culturing cells in serum free medium for the indicated time.

2.3. Cells transfection

STAT1-null BV2 cell line was generated by lentiviral transduction. 293FT cells were co-transfected with STAT1 p84/91shRNA plasmid (Santa Cruz) together with ViraPower Packaging Mix (pLP1, pLP2 and pLP/VSV-G) (Invitrogen, Thermo Fisher Scientific, Eugene, OR, USA). Viral supernatants were collected 72 h later and transducing units/ mL were determined by limiting dilution titration in HCT116 cells. MOI of ~5 was used for BV2 cells transfection. After 5 days of selection with puromycin, STAT1-silenced cells were immediately used for in vitro experiments. 8 µg/mL Polybrene (Sigma-Aldrich) was used to increase transduction efficiency.

4×10^5 BV2 cells were plated in 60-mm plates in DMEM with no antibiotics for transient transfection. After 18 h, the medium was replaced with serum-reduced medium OPTI-MEM (Thermo Fisher Scientific) and the cells were transfected with

wild-type STAT1-pcDNA 3.0 or with C324S STAT1, C492S STAT1 or C324/492S STAT1-pcDNA 3.0 expression vectors and 10 μ L lipofectamine 2000 according to the manufacturer's instructions (Thermo Fisher Scientific). After 18 h, the cells were treated with 1mM diamide for 30 min and 1mM H₂O₂ for 5 min. The cells were harvested and used for analysis of STAT1 phosphorylation by Western blot and for analysis of STAT1 S-glutathionylation by immunoprecipitation.

2.4. Western Blot analysis

Cells were homogenized at 4°C in 20mM HEPES, pH 7.4, containing 420mM NaCl, 1mM EDTA, 1mM EGTA, 1% Nonidet-P40 (NP-40), 20% glycerol, protease cocktail inhibitors (GE Healthcare) and phosphatase cocktail inhibitors. Protein concentration was measured by Bradford reagent (GE Healthcare), using bovine serum albumin as standard. Protein extracts (50 μ g total proteins/lane) were resolved by SDS-PAGE electrophoresis and transferred to PVDF membrane (Immobilon P, Millipore). Immunoblotting assays were carried out by standard procedures using anti-phospho Tyr701-STAT1, anti-STAT1, anti- α Tubulin, anti- β Actin (Santa Cruz Biotechnology), anti-iNOS (Abcam), anti-COX2 (BD biosciences), anti-PARP-1 (Zymed or Santa Cruz Biotechnology). After washing, membranes were developed using anti-rabbit or anti-mouse IgG peroxidase-conjugated antibody (Cell Signaling Technology) and chemiluminescent detection system (Immun-Star WesternC Kit, Bio-Rad). Blotted proteins were detected and quantified using the ChemiDoc XRS Imaging System (Bio-Rad).

2.5. Electrophoretic Mobility Shift Assay (EMSA)

After 4 h starvation, 3×10^6 BV2 cells were treated with 1mM diamide for 30 min or 1mM H₂O₂ for 5 min. LPS treatment (100ng/mL, 4h) was used as positive control for STAT1 activation. Nuclear extracts from BV2 cells were prepared in the presence of 10 μ g/mL leupeptin, 5 μ g/mL antipain, 5 μ g/mL pepstatin, and 1mM phenylmethylsulfonyl fluoride (PMSF). 8 μ g of nuclear extracts were incubated with $2-5 \times 10^4$ cpm of ³²P-labeled double-stranded oligonucleotides of the consensus STAT1 DNA binding site (sis-inducible factor-binding recognition element,

SIE/m67) from the c-fos promoter (5'-gtcgaCATTTCCTCCGTAAATCg-3'), in a 15 μ L reaction mixture containing 20mM Hepes pH 7.9, 50mM KCl, 0.5mM DTT, 0.1mM EDTA, 2 μ g of poly (dI-dC), 1 μ g of salmon sperm DNA, and 10% glycerol. Products were separated on a non-denaturing 5% polyacrylamide gel. The gels were dried and autoradiographed and the intensity of hybridization was quantified using the public domain NIH Image 1.61 program (developed at the U.S. National Institutes of Health and available on <http://rsb.info.nih.gov/nih-image/>).

2.6. Immunoprecipitation and identification of glutathionylated proteins

BV2 cells were lysed in RIPA buffer (20mM Tris-HCl pH 8.0, 150mM NaCl, 1% Nonidet P-40, 1mM EDTA, 10% glycerol, 100mM NaF, 1mM Na₃VO₄) supplemented with protease cocktail inhibitor for 30 min on ice. The same amount of proteins from the clarified cell lysates were incubated with anti-STAT1 antibody overnight at 4°C with rotation. The immune complexes were collected by addition of Protein A sepharose (GE Healthcare), properly washed, eluted in a non-reducing sample buffer (62.5mM Tris HCl pH 6.8, 10% glycerol, 5% SDS, 0.05% bromophenol blue) and separated through a 5% SDS–polyacrylamide gel. After electrophoresis, proteins were blotted onto a PVDF membrane and non-specific binding was prevented by blocking in 5% BSA diluted in tris-buffered saline with Tween 20 (TBST). Then, membranes were probed with primary monoclonal antibody against GSH (ViroGen) and, after washing, blots were incubated with anti-rabbit IgG peroxidase-conjugated antibody (Cell Signaling Technology). Protein-antibody reactions were detected with chemiluminescent detection system (Immun-Star™ WesternC™ Kit, Bio-Rad) using the ChemiDoc XRS Imaging System (Bio Rad). After stripping, membranes were re-hybridized with rabbit anti-STAT1 antibody (Santa Cruz Biotechnology).

2.7. Modified Biotin switch assay

The modified biotin switch assay was performed as described by Butturini et al. [145]. Cells, lysed in RIPA buffer, were treated with the indicated concentrations of H₂O₂

or diamide followed by desalting with Amicon® Ultra (Millipore). The remaining free thiols are blocked by alkylation with 50mM N-ethylmaleimide (NEM) for 20 min on ice, while the glutathionylated thiols were selectively reduced with 60mM DTT for 20 min on ice. After a second desalting step, the cell lysates were treated again with the indicated concentrations of H₂O₂ or diamide that oxidize the free thiols and, thereafter, proteins were incubated with 1mM biotinylated glutathione ethyl ester (BioGEE, Thermo Scientific Pierce). Following one last desalting step, biotinylated proteins were identified with streptavidin-agarose and eluted from the beads with a reducing sample buffer (62.5mM Tris-HCl pH 6.8, 10% glycerol, 5% SDS, 0.05% bromophenol blue, β-mercaptoethanol) and separated through a 7.5% SDS–polyacrylamide gel. After electrophoresis, proteins were blotted onto a PVDF membrane and probed with monoclonal antibody against STAT1.

2.8. Apoptosis hallmarks identification by flow cytometry

BV2 cells were treated for 16 or 24 hours with 1mM H₂O₂ and the apoptotic hallmarks were analyzed by flow cytometry. Cells were washed with phosphate buffered saline (PBS, Thermo Fisher Scientific) and double-stained with Annexin-V-FITC (AnxV) (Miltenyi Biotec) for 15 min and propidium iodide (PI) (Thermo Fisher Scientific) immediately before acquisition on a Fluorescence-activated cell sorting (FACS) Calibur cytometer (Becton Dickinson). PI has an elevated affinity for double-strand nucleic acids but it is not able to enter through unimpaired plasma membrane and it is considered a late apoptosis marker. Annexin-V, instead, is an early apoptosis marker. It binds the phosphatidylserine when it flips from the inner to the outer leaflet of the plasma membrane. Fluorescence signals were detected on FL-1 for Annexin-V and on FL-3 for PI.

2.9. Immunofluorescence and confocal analysis

BV2 microglial cells were seeded onto glass slides and, after treatments, fixed with 4% paraformaldehyde (PFA) for 10 min. SH-SY5Y neuroblast-like cells were plated onto glass slides previously coated with 50µg/mL poly-Lysine and, after treatments, fixed with 4% PFA for 10 min. Fixed cells were permeabilized with 0.1% Triton X-100 in

PBS for 5 min and blocked with 5% bovine serum albumin (BSA) for 1 h. The permeabilization step were not performed if Annexin-V antibody is used. Then, samples were incubated with primary antibodies overnight at 4°C. The following primary antibodies were used: anti-rat CD68 (1:250, Abcam), anti-rabbit iNOS (1:100, Abcam), anti-mouse pTyr701-STAT1 (Santa Cruz Biotechnologies), anti-Annexin V biotin-X conjugate. After incubation, cells were washed three times for 3 min with PBS, incubated with respectively secondary antibody (Alexa Fluor® 488 anti-rabbit, and Alexa Fluor® 594 anti-rat, Alexa Fluor® 568, Alexa Fluor® 633 Streptavidin conjugate, Thermo Fisher Scientific) for 1 h at room temperature, and counterstained with 4',6-diamidino-2-phenylindole (DAPI, 1:1000, Thermo Fisher Scientific) for 15 min at room temperature. Cell images were captured using a confocal laser-scanning fluorescence microscope Leica SP5 (Leica Microsystem) at 40X magnification and processed using Adobe Photoshop and ImageJ software (Rasband, W.S., ImageJ, U. S. National Institute of Health, Bethesda, Maryland, USA, <http://rsb.info.nih.gov/ij/>, 1997–2008).

2.10. Measurement of intracellular reactive oxygen species

ROS production in BV2 cells were quantified with cell-permeant probe 5-(and-6)-chloromethyl-2'7'-dichlorodihydrofluorescein diacetate acetyl ester (CM-H₂DCFDA; Molecular Probes). BV2 microglial cells were seeded in 96-well plate and grown until reaching 90% confluence. Cells were serum starved for 2 hours before addition of 10µM of CM-H₂DCFDA to each well and incubated for 1 hour prior to stimulation with hypoxia for the indicated time. The fluorescent intensity was measured with a multi- mode plate reader (Ex485 nm and Em535 nm) (GENios Pro, Tecan). Fluorescence intensity was compared to control wells for statistical analysis.

2.11. Measurement of nitrite and nitrate

BV2 cells were seeded at the density of $2,5 \times 10^4$ cells/well in 96-well plate and let to adhere overnight. Thereafter, cells were exposed to 1% O₂ for 18 and 24 hours using the hypoxic chamber. After treatment, culture medium were saved for the measurement of nitrite/nitrate (NO₂⁻/NO₃⁻). The NO₂⁻/NO₃⁻ quantification was performed using the NO₂⁻/NO₃⁻ Colorimetric Assay Kit (Cayman Chemical, Ann

Arbor, MI). The nitrite concentration in the cells medium was measured according to the Griess reaction and the calculated concentration was considered as indicator of NO production.

2.12. Cross-talk *in vitro* cellular model

Cross-talk *in vitro* cellular model was performed using SH-SY5Y cells treated with medium conditioned by BV2 cells.

1.5×10^6 BV2 cells were seeded in 10-cm plates in RPMI complete medium and let to adhere overnight. After 2 hours of starvation in serum deprived medium, BV2 cells were exposed to 1% O₂ for 24 hours in the hypoxic chamber in presence or absence of 50μM Myr pretreatment for 30 min. BV2 cells cultured in normoxia were used as negative control. SH-SY5Y cells were seeded at a density of 2.5×10^5 cells/plate in 60-mm plates in complete DMEM and grown for 48 hours. The conditioned media obtained from BV2 plates, Normoxia BV2 conditioned medium (N-BV2-CM), Hypoxia BV2 conditioned medium (H-BV2-CM) and Myr + Hypoxia BV2 conditioned medium (Myr+H-BV2-CM) were collected, centrifuged and immediately used to treat SH-SY5Y cells for the indicated time in hypoxia chamber. BV2 cells pellets, relating to each BV2-CM, were collected and, after lysis, the derived protein extracts were analyzed by Western Blot in order to check the iNOS expression level. SH-SY5Y cells viability was assessed by manual counting viable and death cells, discriminated after Trypan blue staining, using the Neubauer chamber. Cells viability (%) was expressed as percentage of the number of viable cells versus the total amount of cells in each sample.

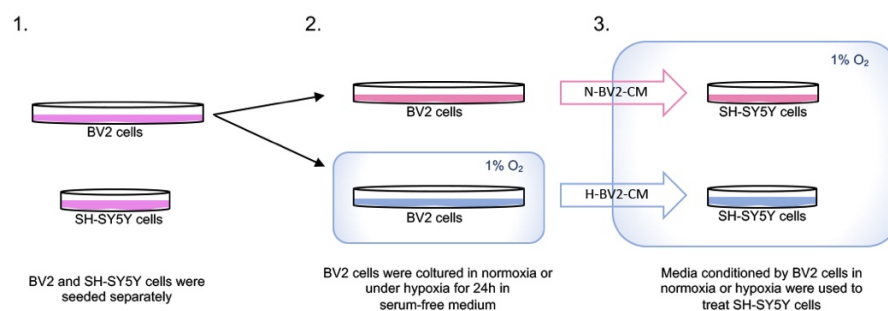


Figure 11. Cross-talk *in vitro* cellular model. 1) BV2 and SH-SY5Y cells were seeded separately and let grow for 24 or 48 hours in normoxia. 2) BV2 cells were cultured under

normoxia or hypoxia for 24 hours in serum-deprived medium. 3) Media conditioned by BV2 cells were collected, centrifuged and immediately used to treat SH-SY5Y cells for the indicated time in hypoxia chamber.

3.13. Statistical analysis

Data are reported as means \pm SEM of independent experiments; statistical analyses were performed using Student's t test. The level of statistical significance was set at $P < 0.05$.

3. Results

3.1. Oxidative stress induces the S-glutathionylation of STAT1 and activates its signaling cascade in BV2 cells

3.1.1. Oxidative stress induces phosphorylation of STAT1 in BV2 cells

The redox regulation of the transcriptional factor STAT1 was examined in murine microglia BV2 cell line after treatment with two physiological oxidative agents: H₂O₂ and GSSG which is involved in regulation of intracellular redox potential. The cells were also treated with the chemical thiol oxidant agent diamide, as positive control for protein S-glutathionylation, and with LPS as positive control for STAT1 Tyr-phosphorylation.

Firstly, BV2 cells were treated with 1mM H₂O₂ for different times and the Tyr701 phosphorylation of STAT1 in whole protein extracts was analyzed by Western Blot using a specific antibody. As shown in figure 12A, 1mM H₂O₂ treatment rapidly leads to the tyrosine phosphorylation of STAT1 with the maximum activation at 5 min. The membrane was also incubated with anti-STAT1 antibody in order to check the loading of samples. Tyr701 phosphorylation of STAT1 induced by 4 hours treatment with 100 ng/mL LPS is reported as positive control.

To evaluate the ability of other oxidants to phosphorylate STAT1, the cells were treated with 1mM GSSG or 1mM diamide for 30 min. As shown in figure 11B, the diamide treatment induces Tyr701 phosphorylation of STAT1. Conversely, GSSG treatment does not induce protein phosphorylation. The membrane was also incubated with anti-STAT1 antibody in order to check the loading of samples (Fig.12B).

In order to verify STAT1 functional activation, its DNA binding activity was examined by EMSA. As shown in Fig.12C, the treatment of BV2 cells with these oxidants were able to induce the DNA-binding activity of STAT1 in BV2 cells.

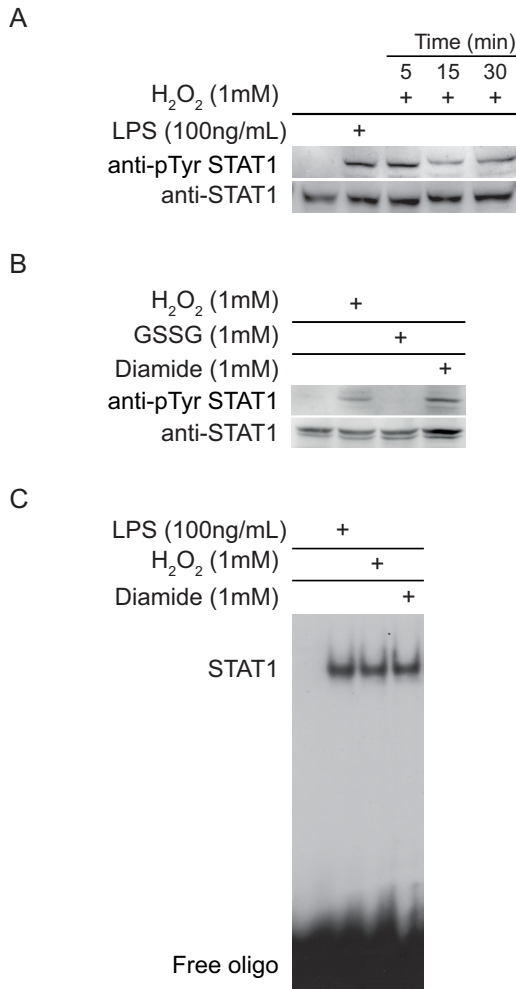


Figure 12. Oxidative stress induces the activation of STAT1 in BV2 cell line. A) Western Blot analysis shows that 1mM H₂O₂ increase STAT1 Tyr701 phosphorylation after 5 min in BV2 cells. Treatment with 100ng/mL LPS for 4h is used as positive control of STAT1 signaling activation. The total amount of STAT1 is not affected during the experiments. B) Western Blot analysis shows that 1mM H₂O₂ after 5 min or 1mM diamide after 30 min increase Tyr701 phosphorylation of STAT1 in BV2 cell line. The treatment with 1mM GSSG is unable to induce STAT1 Tyr701 phosphorylation. The blot exhibits equivalent levels of STAT1 in all lanes. C) EMSA analysis shows the increased ability of STAT1 to bind DNA after cells treatment with 1mM H₂O₂ for 5 min or 1mM diamide for 30 min. Treatment with 100ng/mL LPS for 4 hours was used as positive control. The figure represents the result of four separate experiments.

3.1.2. Oxidative stress induces S-glutathionylation of STAT1 in BV2 cells

S-glutathionylation of cysteine residues is a reversible post-translational modification involved in protein redox regulation [146], [147]. In order to analyse the molecular mechanism of STAT1 phosphorylation under oxidant treatment, STAT1 was immunoprecipitated from protein extracts of oxidant-treated BV2 cells using anti-STAT1 antibody, and S-glutathionylation was analysed by Western Blot under non-reducing condition with anti-GSH antibody.

Figure 13A shows that both H₂O₂ and diamide treatments induce STAT1 S-glutathionylation whereas GSSG does not induce protein modifications. Additionally, treating immunoprecipitated STAT1 with 20mM DTT, the glutathionylation signal is

totally extinguished. This last step of reduction proved the reversibility of the modification (Fig. 13A).

Moreover, the modified biotin switch assay on STAT1 was performed. BV2 cells were treated with biotinylated glutathione and the modified proteins isolated by affinity with streptavidin-conjugated media. As expected, STAT1 was modified with biotinylated glutathione in BV2 cells treated with 1mM H₂O₂ or 1mM diamide, proving the presence of reactive thiol groups involved in S-glutathionylation in response to oxidative stimuli (Fig. 13B).

These results show that treatment of BV2 cells with either H₂O₂ or diamide is associated with enhanced oxidative modification of STAT1 by glutathionylation.

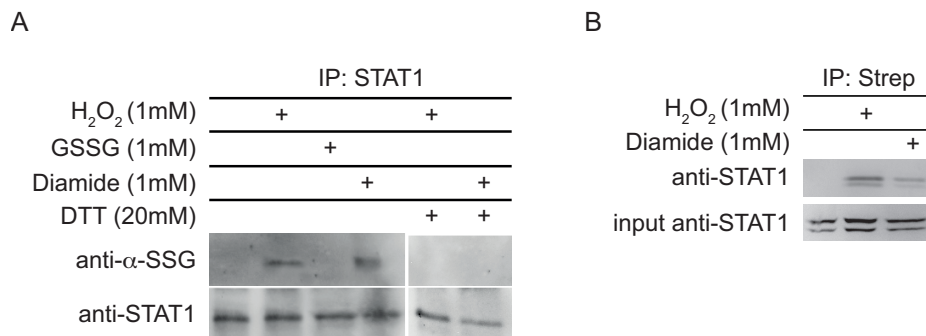


Figure 13. Oxidative stress induces S-glutathionylation of STAT1 in BV2 cell line.

A) Western Blot analysis of immunoprecipitated STAT1 (IP: STAT1) shows that treatment with 1mM H₂O₂ for 5 min or 1mM diamide for 30 min increase the amount of S-glutathionylated STAT1. Treatment with 1mM GSSG for 30 min does not induce any modification of STAT1. This post- translational modification is completely reversed by 20mM DTT treatment. B) STAT1 post-translational modifications in BV2 cells are analyzed by Biotin Switch assay followed by streptavidin immunoprecipitation (IP: Strep) and by Western Blot analysis with anti-STAT1 antibody. S-glutathionylated STAT1 is detected in cells after treatment with 1mM H₂O₂ (5 min) or 1mM diamide (30 min). The images are representative of four experiments performed separately.

3.1.3. Cys324 and Cys492 are targets of S-glutathionylation of STAT1 in BV2 cells

Recently, it has been demonstrated that Cys324 and Cys492 residues are S-glutathionylated in recombinant purified form of STAT1 under oxidative stress [148]. In order to confirm the involvement of these cysteine residues in redox regulation of STAT1 signaling in cells, STAT1-null BV2 cells were transfected with wild-type (WT)

STAT1, C324S and C492S single mutants or C324/492S double mutant and treated with 1mM H₂O₂ for 5min. The protein extracts were analyzed by Western Blot under non reducing condition using anti-phosphoTyr701-STAT1 antibody. As shown in Fig 14A, STAT1 was phosphorylated in STAT1-null BV2 cells transfected with WT or single mutants (Fig.14A, lane 2 and lanes 3, 4 respectively) whereas it is not modified in cells expressing C324/492S STAT1 double mutant (Fig.14A, lane 5). EMSA analysis of protein nuclear extracts from the same transfected cells, demonstrated that H₂O₂ treatment increased DNA binding activity of WT STAT1 (Fig.14B, lane 2) whereas was not able to induce DNA binding activity in single or double STAT1 mutants (Fig.14B, lanes 3, 4 and 5).

These data indicate that S-glutathionylation of Cys324 and Cys492 residues of STAT1 did not impair either phosphorylation or DNA binding under oxidative stress, suggesting a putative regulatory role for this modification.

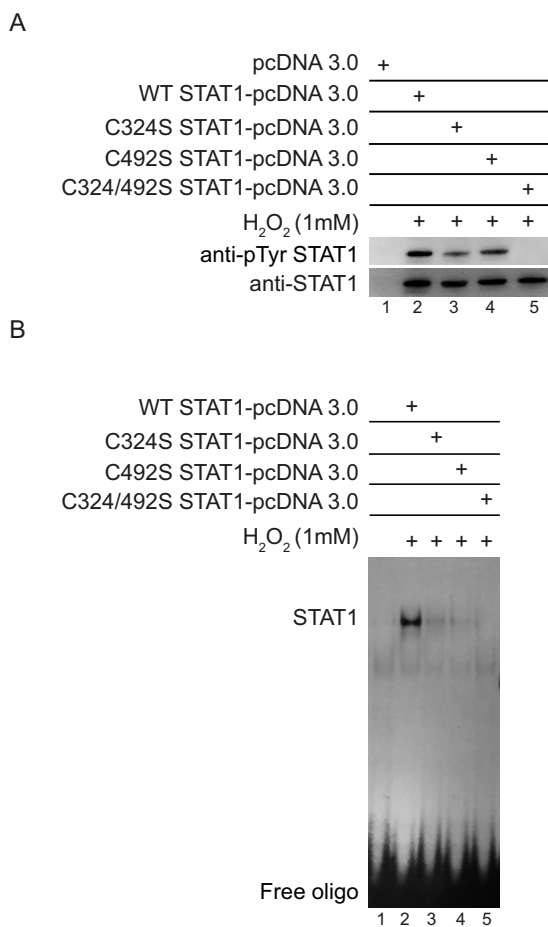


Figure 14. H₂O₂ treatment and phosphorylation of WT STAT1 and mutants STAT1 in STAT1- null BV2 cells.

Protein extracts were prepared from STAT1-null BV2 cells transfected with WT, C324S, C492S or C324/492S STAT1 after treatment with 1mM H₂O₂ for 5 min. A) Western blot analysis of whole protein extracts exhibits that H₂O₂ treatment induces Tyr701 phosphorylation of WT STAT1 (lane 2) and of the STAT1 single mutants as well (lanes 3 and 4), whereas it was not able to induce Tyr701 phosphorylation of STAT1 double mutant (lane 5). The blot shows equivalent STAT1 levels in all samples. B) EMSA analysis of nuclear protein extracts from transfected BV2 cells shows that treatment with H₂O₂ increased DNA-binding activity of STAT1 in WT STAT1 transfected cells (lane 2) whereas was not able to induce DNA binding activity in single or double STAT1 mutants transfected ones (lanes 3, 4 and 5). The images are representative of four experiments performed independently.

3.1.4. Oxidative stress induces apoptosis in BV2 cells

The effect of oxidative stress on BV2 cells was evaluated monitoring cells viability with Trypan Blue assay and the Countess® automated cells counter. Cells viability decrease to $30.0 \pm 2.6\%$ in a time dependent manner as consequence of the treatment with 1mM H_2O_2 for 24 hours. With the purpose to assess the role of STAT1 signaling in microglia cells death under oxidative stress, the same treatment was performed on STAT1-null BV2 cells. The viability of STAT1-null cell line was less but significantly affected by 1mM H_2O_2 compared to that of BV2 cells (Fig.15), stating that the transcriptional factor STAT1 is partially involved in cell death induced by oxidant agents.

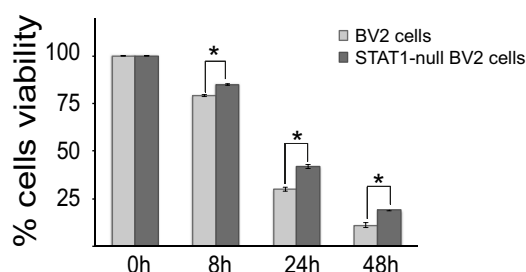


Figure 15. BV2 cells and STAT1-null BV2 cells viability after H_2O_2 treatment. Cells were treated with 1mM H_2O_2 for 8, 16, 24 and 48 hours and viability was evaluated by Trypan Blue exclusion test. The graph shows that H_2O_2 treatment decrease BV2 and STAT1-null BV2 cells viability in a time dependent manner. STAT1-null BV2 cells viability is significantly less affected by the treatment compared to BV2 cell. * $P < 0.05$. The results presented are the means \pm SEM of at least six independent experiments.

In order to investigate the molecular mechanism of cell death, BV2 cells treated with 1mM H_2O_2 were analysed with Annexin V-FITC/PI double staining followed by flow cytometry assay. More than 40% of treated cells show Annexin V-positive/PI-negative staining at 16 hours revealing the onset of the apoptosis process (Fig.16A). Confocal microscopy analysis using Annexin-V staining revealed the phosphatidylserine shift from the inner to the outer side of the cytoplasmic membrane confirming the apoptotic death (Fig.16B). Moreover, the cell nuclei stained with DAPI showed the morphological changes related to the apoptotic process. Finally, in order to confirm the cell death mechanism proposed, the presence of PARP cleavage was investigated by Western Blot analysis (Fig.16C).

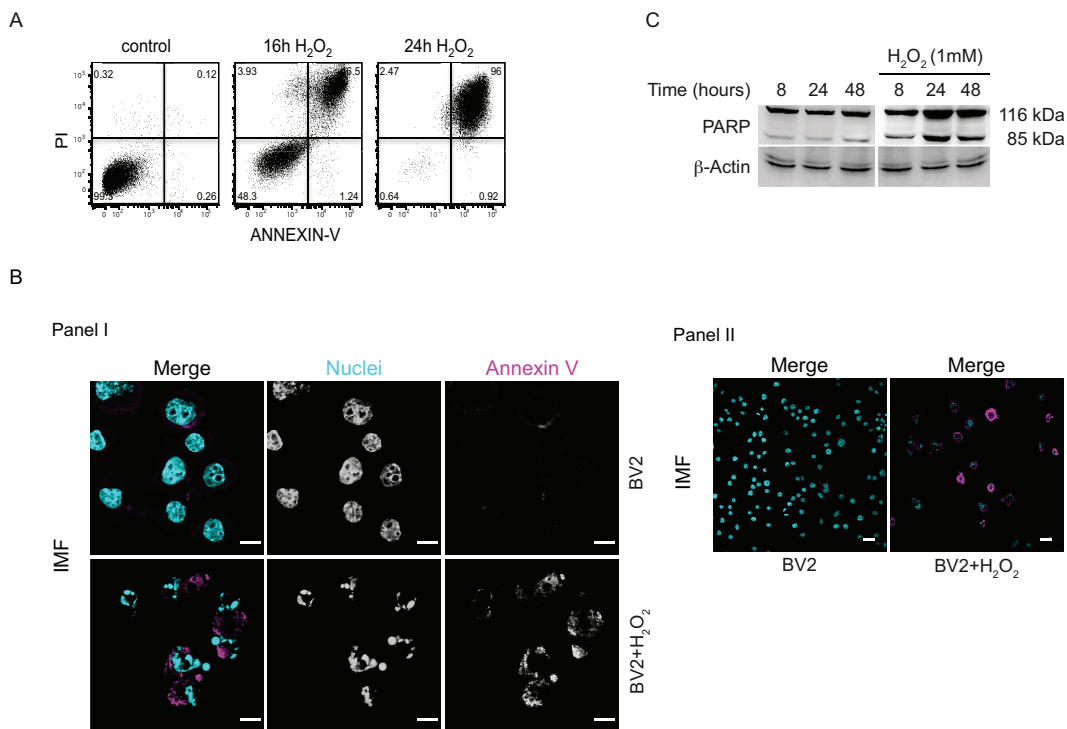


Figure 16. Analysis of apoptotic hallmarks in BV2 cell line after H₂O₂ treatment. A) Analysis by Flow Cytometry shows the time-dependent progression of apoptosis. Cells were stained with AnxV and PI to distinguish unaffected cells (AnxV^{neg} PI^{neg}), early apoptosis (AnxV^{pos} PI^{neg}) and late apoptosis (AnxV^{pos} PI^{pos}) by flow cytometer. B) BV2 cells, treated with 1mM H₂O₂ for 16 hours, were stained with Annexin-V (magenta) and DAPI (cyan). Panel I: the top line shows untreated BV2 cells and the bottom line shows BV2 cells treated with H₂O₂ using lens 63X. Scale bars: 10 μm. Panel II: Images representing untreated and 1mM H₂O₂ treated for 16 hours BV2 cells using lens 40X. Scale bars: 50μm. C) Western Blot analysis shows PARP cleavage induced by H₂O₂ in a time dependent manner. β-actin was used as loading control. The images are representative of four experiments performed independently.

3.2. M1 microglia activation under hypoxia: the key role of STAT1

Cerebral hypoxia has been found to be strictly correlated to the onset of neuroinflammatory process in pathologies like Alzheimer's, Parkinson's and Huntington's diseases, amyotrophic lateral sclerosis and cerebrovascular diseases [149]. Indeed, microglia cells under hypoxia condition shift towards M1 polarization phenotype triggering and exacerbating the inflammatory process [150].

3.2.1. Hypoxia induces phosphorylation of STAT1 in BV2 cells

To determine if hypoxia stimulus affects STAT1 signaling, BV2 cells were exposed to 1% O₂ for 0.5, 1, 2, 4 and 18 hours in hypoxic chamber. The protein extracts were tested by Western Blot using specific antibody directed toward Tyr701-phosphorylated STAT1. As shown in figure 17, the levels of Tyr701-phosphorylated STAT1 were transiently increased by hypoxia, peaking after 2 hours of treatment. Exposure to hypoxia did not alter the total level of STAT1 protein (Fig.17).

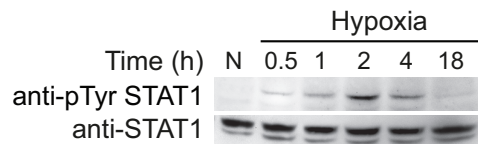


Figure 17. Hypoxia triggers STAT1 activation in BV2 cells. Western Blot analysis shows that STAT1 Tyr701 phosphorylation transiently increases, peaking after 2 hours, in BV2 cells exposed to hypoxia. Increased phosphorylation was detected within 30 min of hypoxia treatment and was sustained up to 4 hours after stimulation. The total amount of STAT1 is not affected during the experiments. The images are representative of four experiments performed independently.

As expected, the analysis by confocal microscopy reveal that pTyr701-STAT1 traffics from the cytoplasm to the nucleus in most of BV2 cells at 2 hours under hypoxia (Fig.18).

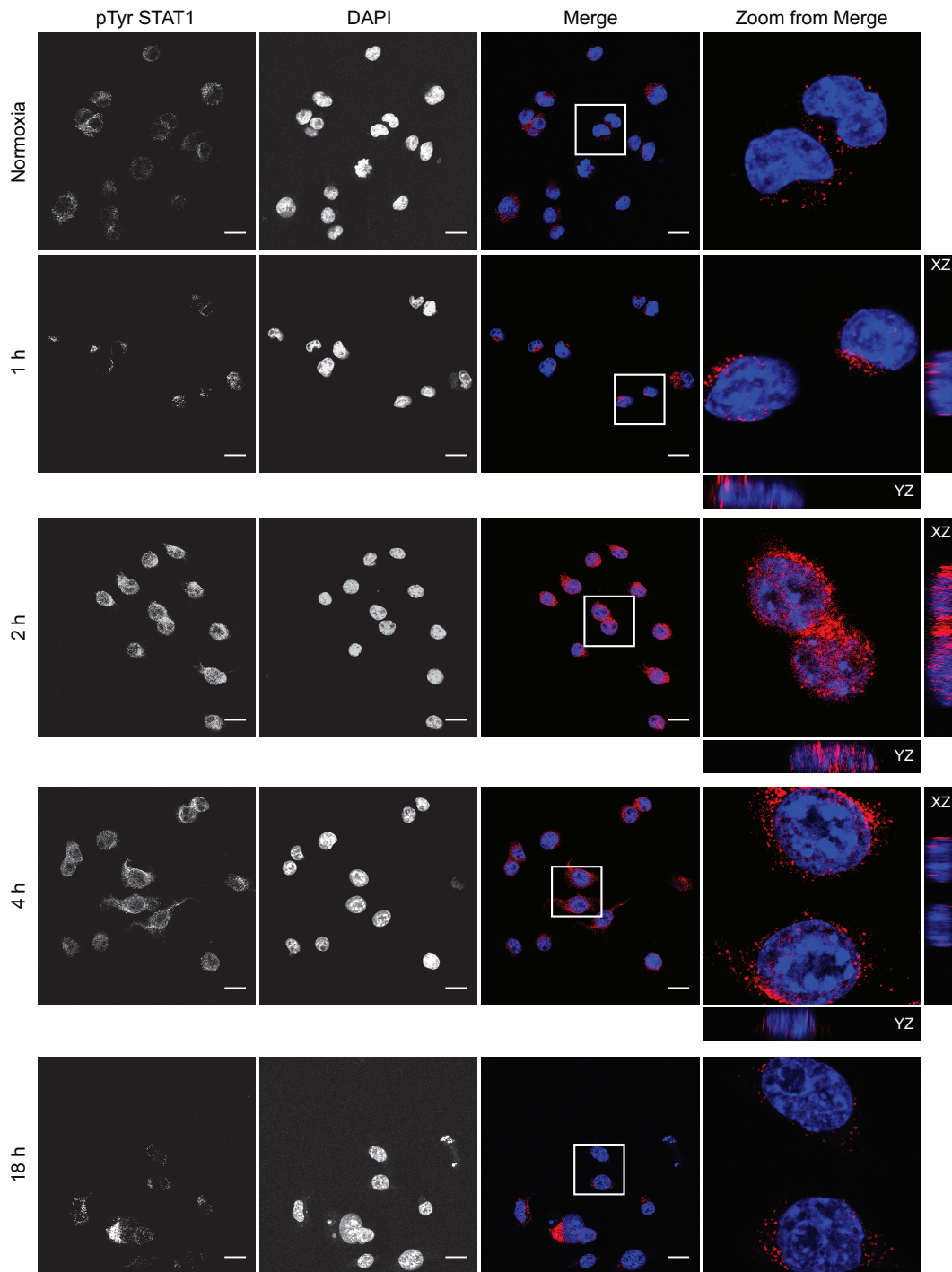


Figure 18. Hypoxia triggers STAT1 activation in BV2 cells. BV2 cells cultured under 1%O₂ for the indicated time have been immuno-stained with phosphoTyr701 STAT1 (red) and analyzed by confocal microscopy (Lens 40X). Nuclei were stained with DAPI (blue). Scale bars: 50 μ m. The images are representative of four experiments performed independently.

3.2.2. Hypoxia induces S-glutathionylation of STAT1 in BV2 cells

In order to study the effect of hypoxia on intracellular redox state, BV2 cells were treated with CM-H₂DCFDA, a specific cell-permeant ROS probe, and cultured under hypoxia for the indicated times. The fluorescence intensity of cells increased in a time-dependent manner peaking after 4 hours of treatment. These data suggested that hypoxia treatment increases intracellular ROS levels (Fig.19).

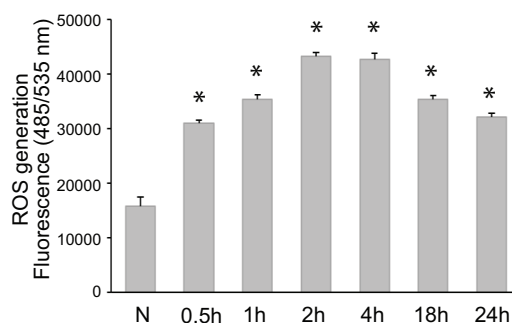


Figure 19. Hypoxia affects the intracellular redox state. BV2 cells treated with CM-H₂DCFDA were cultured for the indicated time under 1% O₂. The fluorescent intensity measured indicates the intracellular ROS production (Ex485 nm and Em535 nm). BV2 cells cultured under normoxic condition were used as control (N). The results presented are the means \pm SEM of at least six independent experiments. *P < 0.01 in comparison with control cells under normoxia.

The oxidative stress induces modifications on sensitive thiol groups of cysteine residues and modulates proteins folding and interactions changing their biological function. To investigate the molecular mechanism of hypoxia-induced STAT1 pathway activation, protein extracts from BV2 cells cultured under hypoxia for the indicated times, were immunoprecipitated using anti-STAT1 antibody. Western Blot analysis under non reducing condition revealed that hypoxia treatment time-dependently induced the STAT1 S-glutathionylation with a maximum signal at 4 hours (Fig.20). These data confirm that STAT1 is a redox sensitive protein.

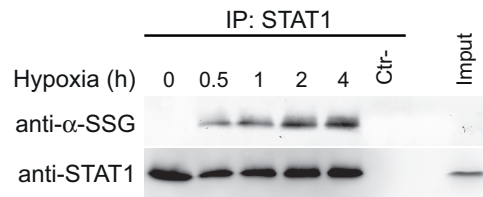


Figure 20. Hypoxia induces S-glutathionylation of STAT1. BV2 cells were treated with hypoxia for the indicated time and STAT1 protein was immunoprecipitated from whole protein extracts using anti-STAT1 antibody. Immunoprecipitated STAT1 (IP: STAT1) was detected by Western Blot under non-reducing condition with anti-SSG and, after membrane stripping, with anti-STAT1 antibody. The same protein extract amount was immunoprecipitated with rabbit IgG and analyzed in Western Blot (Ctrl-). Samples from cells lysates have been saved before pull-down as control (input). The images are representative of four

3.2.3. Hypoxia triggers the transition to M1 phenotype in BV2 cells

The role of hypoxic environment, characterized by the presence of oxidative stress, in inducing the transition of microglia from the “resting” state to the pro-inflammatory M1 phenotype was investigated. BV2 cells were exposed to 1% O₂ for 0.5, 2, 18 and 24 hours using the hypoxic chamber. In accordance with earlier studies, hypoxia (1% O₂) treatment induced morphological changes in BV2 cells towards the typical M1 phenotype already after 1 hour under 1% O₂ (Fig. 21).

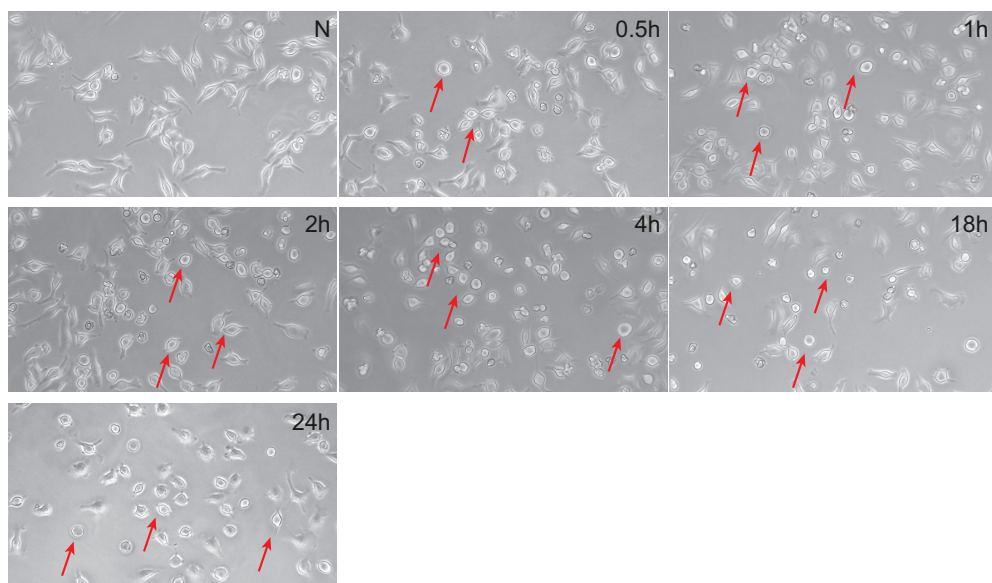


Figure 21. Hypoxia induces M1 phenotype activation in microglia. Analysis by phase-contrast microscopy of BV2 cells exposed to 1% O₂ for 0.5, 1, 2, 4, 18 and 24 hours using the hypoxic chamber. Microglial cells phenotype changes from the ramified to the amoeboid shape, typical of M1 state activation (arrows) (10X). The pictures are representative for three separate experiments.

Moreover, iNOS and COX2 expression, was evaluated as markers of the M1 polarization. Western Blot analysis showed high levels of iNOS and COX2 starting from 18 hours under 1% O₂ (Fig. 22A). As expected, the levels of nitrite and nitrate (NO₂⁻/NO₃⁻), the stable end products of NO, increased in medium of BV2 cells after exposure to hypoxia (Fig. 22B).

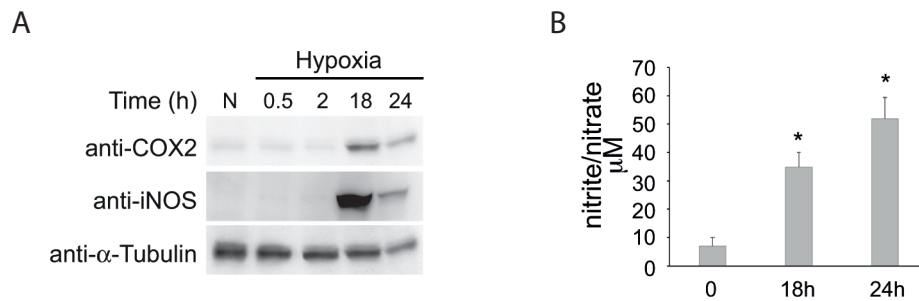


Figure 22. Hypoxia induces M1 phenotype activation in microglia A) Western blot analysis of whole cell extracts shows high levels of iNOS and COX2 starting from 18 hours under 1% O₂. α-Tubulin was used as loading control. B) The culture media of BV2 cells after exposition to 1% O₂ for 18 and 24 hours were saved for the measurement of NO₂⁻/NO₃⁻ by Griess reaction. The graph shows that hypoxia time-dependently increases NO₂⁻/NO₃⁻ concentration in the culture medium of cells. Data are reported as means ± SE of four independent experiments (n= 4); statistical analyses were performed using Student's t test. *p< 0.05 versus normoxic condition.

To confirm the phenotype transition from resting cells to pro-inflammatory microglia, the expression of CD68 and iNOS, M1 markers, were investigated by immunofluorescence in BV2 cell line after 18 and 24 hours hypoxia treatments. As shown in Figure 23, BV2 “resting” cells presents very low number of CD68⁺ cells and low level of iNOS expression. Following hypoxia exposure, the number of CD68⁺ cells increases time-dependently, with widespread expression of iNOS in CD68⁺ cells.

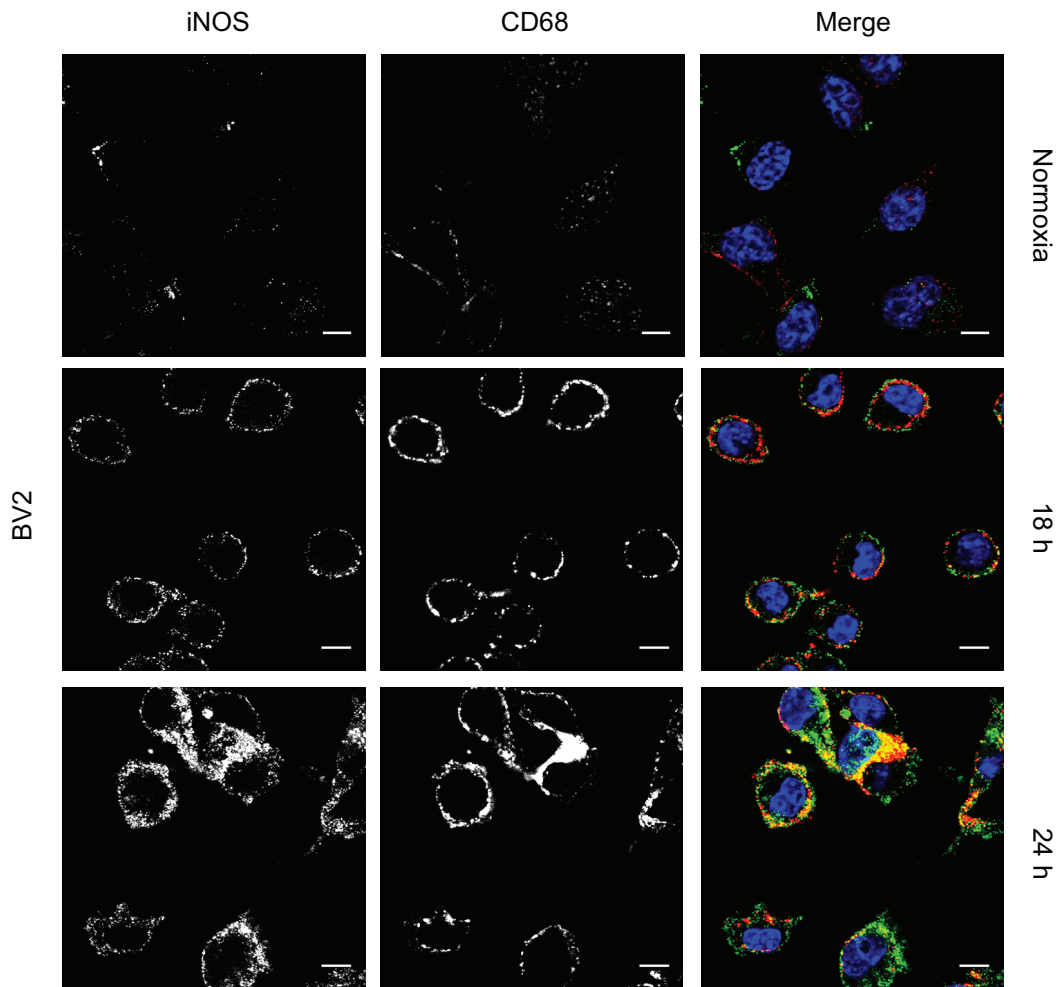


Figure 23. Hypoxia induces M1 phenotype markers expression in microglia. BV2 cells were exposed to 1% O₂ for 18h and 24h, were analyzed by confocal microscopy with CD68 (red) and iNOS (green) antibodies using lens 40x. Cell nuclei were counterstained with DAPI (blue). The images are representative of three separate experiments.

Additionally, to verify the effect of oxidative stress on iNOS expression, BV2 cells were pretreated for 30 min with 5mM or 20mM N-acetylcysteine (NAC), an antioxidant agent, and thereafter, cells were exposed to hypoxia for 18 hours. Western Blot analysis of iNOS expression revealed that NAC prevent iNOS expression in a dose-dependent manner (Fig.24). Then, BV2 cells were pretreated with 0.5mM and 1mM glutathione mono-ethyl-ester (GEE) for 18 hours and were exposed to hypoxia for 18 hours. Western Blot analysis showed iNOS expression levels is reduced in a

dose-dependent manner after GEE pretreatment. (Fig.24). These data confirm the key role of GSH/GSSG redox couple in iNOS regulation.

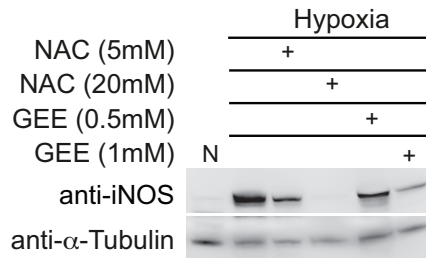


Figure 24. Oxidative stress induces iNOS expression in BV2 microglia. BV2 cells were pretreated with NAC for 30 min or with GEE for 18 hours and then were exposed to hypoxia for 18 hours. iNOS expression in whole protein extracts was analyzed by Western Blot. α -tubulin antibody was used as loading control. BV2 cells cultured under normoxia were used as control (N). Data are representative of five separate experiments.

3.2.4. Hypoxia leads to M1 phenotype activation through the activation of STAT1 signaling in BV2 cells

M1 microglia phenotype involves multiple signaling cascades, among them the NF- κ B family of transcription factors is one of the best characterized [151]. Despite the fact that hyper-activation of STAT1 in glia cells and its contribution to neuroinflammation and neuronal damage are well known, its involvement in the regulation of M1 transition is not completely clarified. In order to understand the role of STAT1 in M1 microglia activation, iNOS expression, the main hallmark of M1 polarization was analyzed in STAT1-null BV2 cells exposed to 1% O₂ for 2, 18 and 24 hours using the hypoxic chamber; BV2 cells cultured under the same conditions were used as comparison. STAT1-null BV2 cells and BV2 cells kept in normoxia were considered as control. STAT1-null BV2 cells under hypoxia showed lower iNOS expression than the parent cells cultured in the same condition (Fig.25).

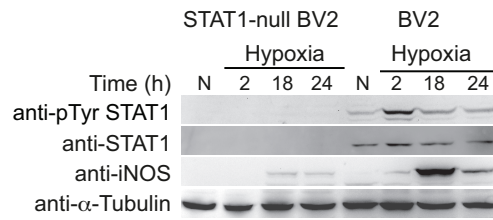


Figure 25. Hypoxia leads to M1 phenotype activation in BV2 cells through the activation of STAT1. BV2 and STAT1-null BV2 cells were cultured under 1% O₂ for the indicated time. The whole protein extracts were analyzed by Western Blot using anti-phosphoTyr701-STAT1 antibody and after membrane stripping, with anti-iNOS antibody. The same blot was incubated with anti-STAT1 antibody. Anti-α-Tubulin antibody was used to verify the amount of loaded proteins. BV2 and STAT1-null BV2 cells cultured under normoxic condition were used as control (N). Images represents the results of four independent experiments.

The cells response to hypoxia was also examined by immunofluorescence. iNOS and CD68 expression was analyzed after 18 and 24 hours under hypoxia. CD68 and iNOS expression levels in STAT1-null cells are less affected by hypoxia treatments (Fig.26) compared to parental cell line (Fig.23).

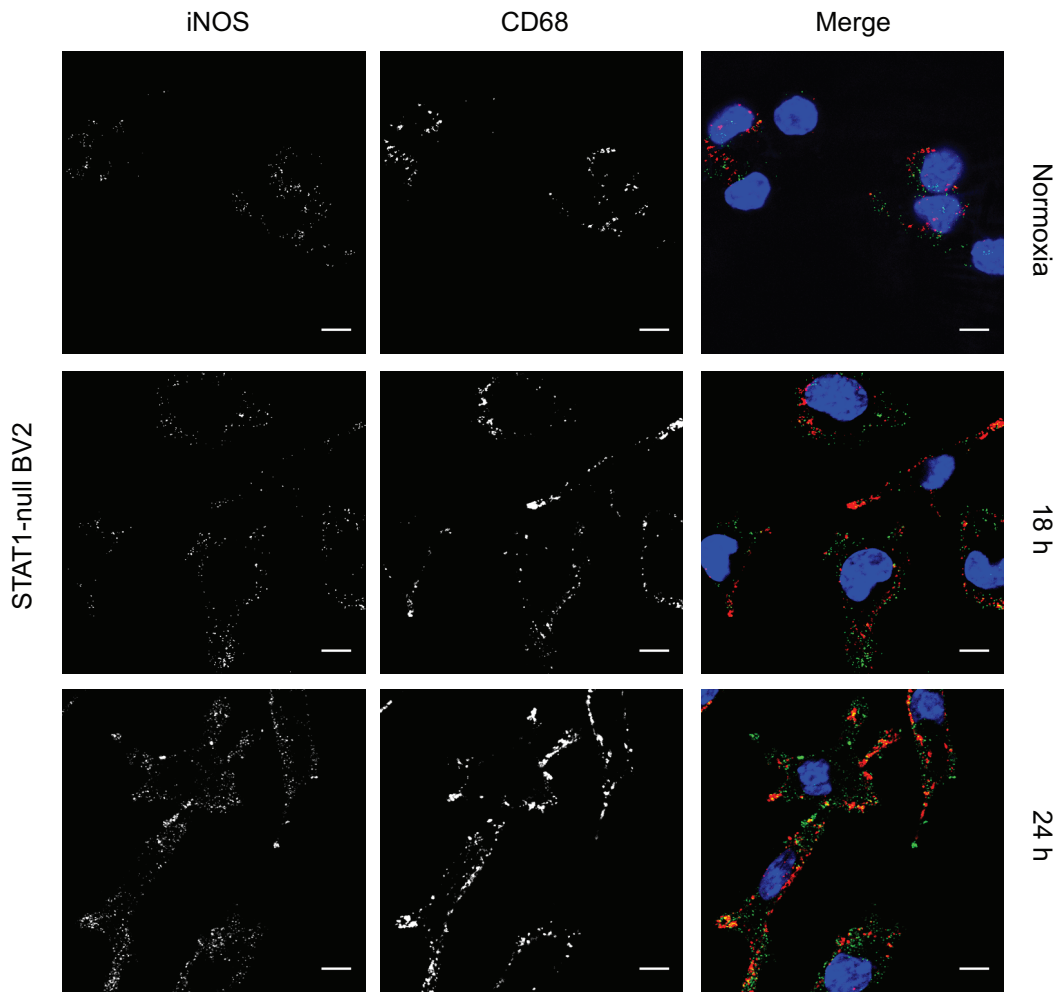


Figure 26. STAT1-null BV2 cells do not express M1 phenotype markers after hypoxia exposure. STAT1-null BV2 cells were cultured under 1% O₂ for 18 and 24 hours. The expression of CD68 (red) and iNOS (green) were analyzed by confocal microscopy (40X lens). Cell nuclei were counterstained with DAPI (blue). Scale bars: 50µm. Images represent the results of three independent experiments.

Altogether these data demonstrate the key role of STAT1 in the transition from “resting” phenotype to M1 proinflammatory polarization in microglia cells under hypoxia.

3.2.5. Hypoxia-activated BV2 cells induce SH-SY5Y cells apoptosis

M1 activated microglial cells release cytokines and growth factors regulating, not only neuronal plasticity and synapse formation, but also neuronal apoptosis [139]. In order to verify the ability of hypoxia-activated BV2 cells to induce neuronal death, the cross-talk between microglia and neurons was studied using the cross-talk *in vitro* model

described in Material and Method Section The viability of both BV2 and SH-SY5Y cell lines separately cultured under 1% O₂ was evaluated in order to exclude the contribution of hypoxia in inducing cellular death (Fig. 27A and 27B, respectively). The viability of SH-SY5Y cells cultured under hypoxia for 6, 18, 24 and 48 hours in presence of H-BV2-CM and N-BV2-CM were compared. As shown in figure 27C, H-BV2-CM time-dependently induces a decrease in SH-SY5Y cells viability (*p<0.005 **p<0.0005). Specifically, after 24 hours SH-SY5Y viability decreases from 92.33±1.33% to 55.00±0.58%.

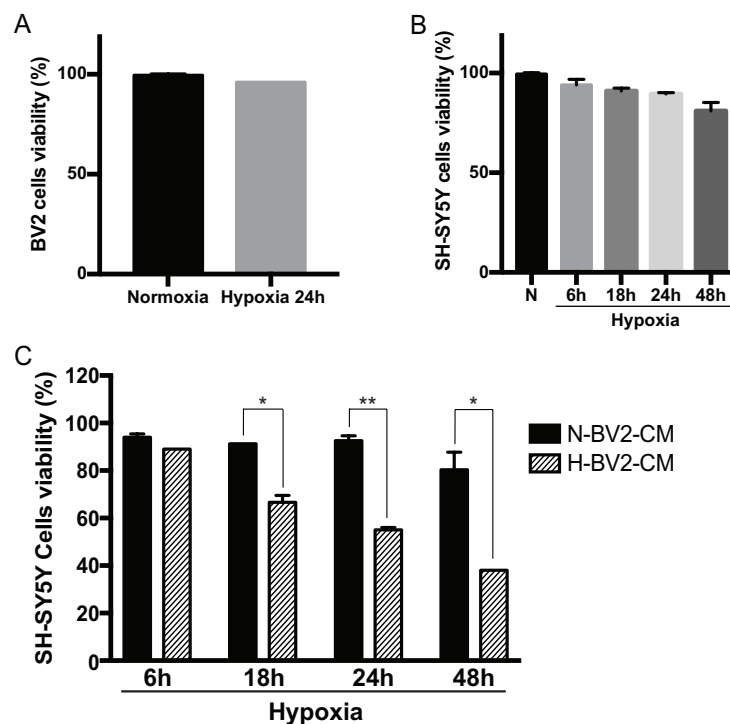


Figure 27. Hypoxia-activated BV2 cells induce SH-SY5Y cells death. A) Viability (%) of BV2 cells cultured under hypoxia for 24hours. Hypoxia does not induce microglia cells death. B) Viability (%) of SH-SY5Y cells cultured in non-conditioned medium under hypoxia for 6, 18, 24 and 48h. Hypoxia does not induce SH-SY5Y cells death. C) Cross-talk between BV2 and SH-SY5Y. Viability (%) of SH-SY5Y cells cultured under hypoxia for 6, 18, 24 and 48h in N-BV2-CM (■) and H-BV2-CM (▨). H-BV2-CM induced a significant decrease in SH-SY5Y cells viability compared to N-BV2-CM. Values represent the mean ± SEM of six separate experiments. *p<0.005; **p<0.0005.

In order to deepen the mechanism of neuronal death induced by hypoxia-activated microglia, some hallmarks of the apoptotic process have been investigated. The phosphatidylserine shift to the outer side of the cytoplasmic membrane on SH-SY5Y

treated with H-BV2-CM was verified by confocal microscopy using Annexin-V staining (Fig.28).

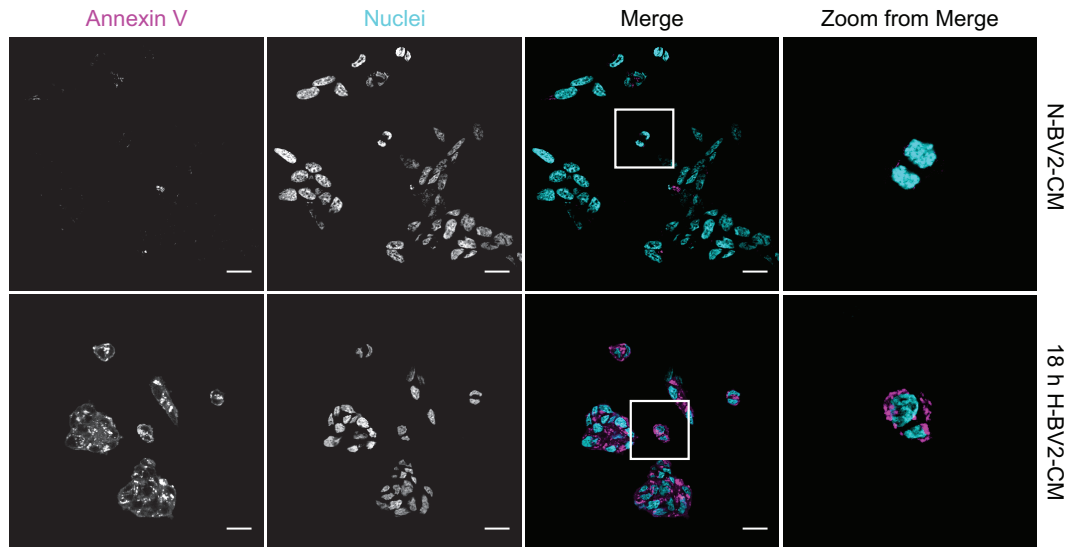


Figure 28. H-BV2-CM induces the exposure of phosphatidylserine residue on the cell surface of SH-SY5Y cells. SH-SY5Y cells were cultured under hypoxia for 18 hours in presence of N-BV2-CM and of H-BV2-CM. The cells were stained with Annexin-V (magenta) and DAPI (cyan) and analyzed by confocal microscopy (40X lens). Scale bar: 50 μ m. Images represents the results of three independent experiments.

Finally, PARP cleavage in protein extracts of SH-SY5Y cells after 48 hours of treatment with H-BV2-CM, confirms the cell death mechanism proposed (Fig.29).

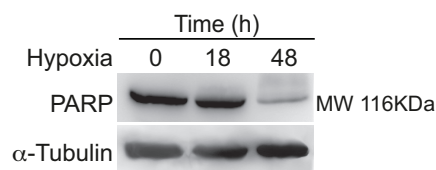


Figure 29. H-BV2-CM induces PARP cleavage in SH-SY5Y cells. SH-SY5Y cells were cultured under hypoxia for 18 and 48 hours in presence of H-BV2-CM and PARP cleavage was analyzed by Western Blot. SH-SY5Y cultured in non-conditioned medium were used as negative control. α -tubulin was used as loading control. Images represents the results of three independent experiments.

3.3. Myricetin counteracts M1 activation of BV2 cells induced by hypoxia

Myricetin (Myr) is a polyphenolic compound belonging to the flavonoid class and it is commonly derived from vegetables and fruits. It is known that Myr, due to its antioxidant activity, is able to act as ROS scavenger and has protective effects against carcinogenesis, inflammation and diabetes [152]. Moreover, Scarabelli et al. demonstrated that Myr is an efficient and highly specific inhibitor of STAT1 signaling pathway through the direct interaction with STAT1 protein [153]. On that basis, it has been evaluated the ability of Myr to counteract the microglia activation induced by hypoxia.

3.3.1. Myricetin counteracts M1 phenotype activation induced by hypoxia in BV2 cells

In order to evaluate the ability of Myr to inhibiting the expression of the typical inflammatory markers of microglia activation, murine microglia BV2 cells were pretreated with 25, 50 and 75 μ M Myr for 30 min and, afterwards, the cells were exposed to 1% O₂ for 18 hours using the hypoxic chamber. The iNOS and COX2 expression in protein extracts from BV2 cells were evaluated by western blot using antibodies specific for the indicated markers. The blot analysis shows that Myr is able to inhibit the hypoxia-induced expression of both markers in a dose-dependent manner (Fig.30). Anti- β -actin antibody was used to check the proteins loading.

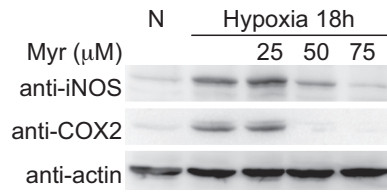


Figure 30. Myr counteracts the hypoxia-induced iNOS and COX2 expression in BV2 cells. BV2 cells were pretreated with 25, 50 and 75 μ M Myr for 30 min and the cultured under 1 % O₂ for 24 hours. The whole protein extracts were analyzed by Western Blot using anti-iNOS and anti-COX2 antibodies. Anti- β -actin antibody was used on the same blot as protein loading control. BV2 cells cultured under normoxic condition were used as negative control (N). Images represents the results of four independent experiments.

Furthermore, the expression of CD68 and iNOS were investigated by confocal microscopy in BV2 cells pretreated for 30 min with 50 μ M Myr and exposed to hypoxia for 24 hours. BV2 resting cells cultured in normoxia were used as control. As shown in figure 31, BV2 cells pretreated with Myr before the 1% O₂ treatment express much lower levels of CD68s and of iNOS compared to BV2 cells without Myr pretreatment. These data confirm that myricetin is capable to prevent hypoxia-induced microglia activation through the inhibition of STAT1 signaling pathway.

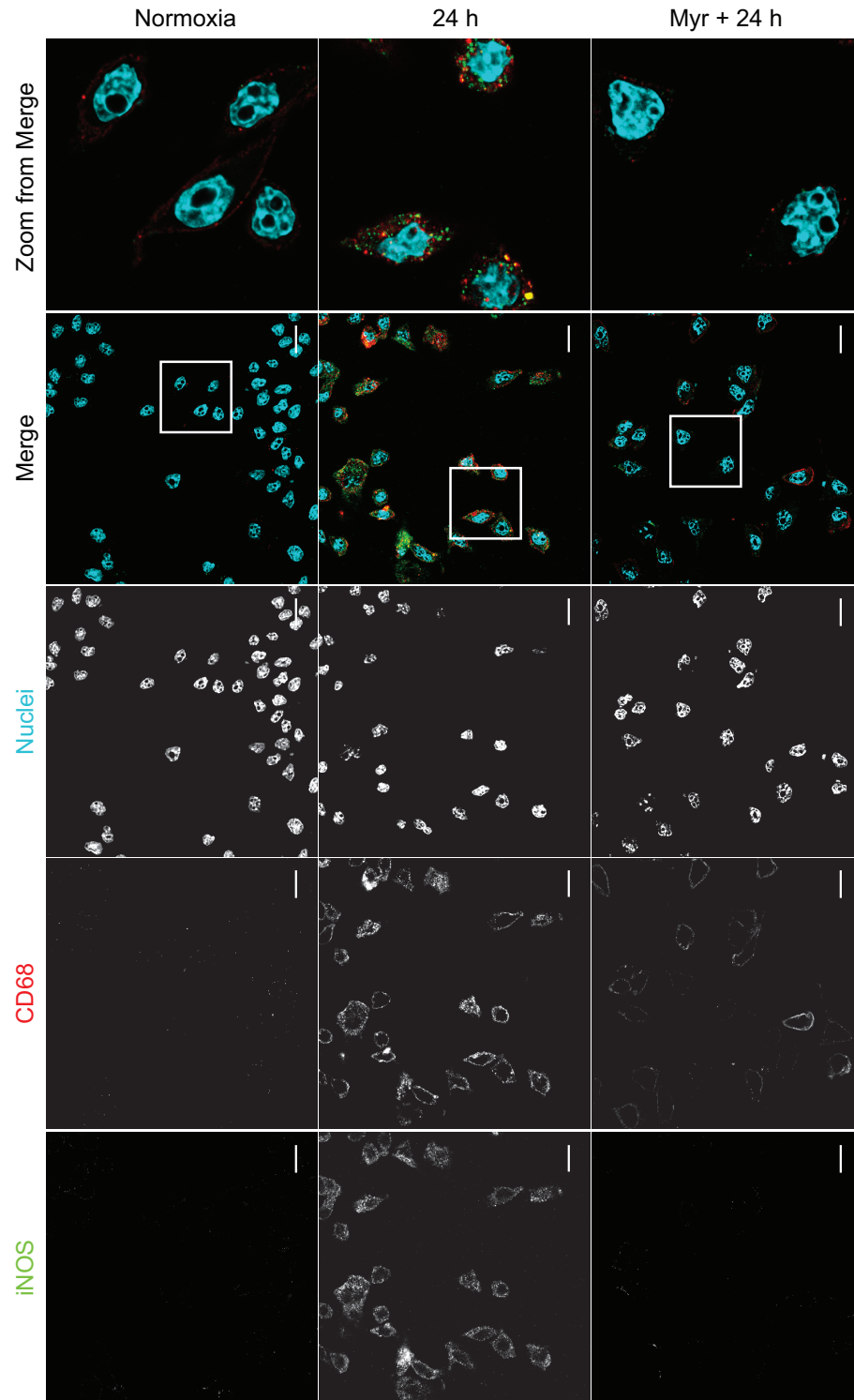


Figure 31. Myr counteracts the hypoxia-induced iNOS and CD68 expression in BV2 cells. BV2 cells, pretreated with 50 μ M Myr for 30 min or not, were exposed to 1% O₂ for 24 hours. The cells were immunostained with CD68 (red) and iNOS (green) and analyzed by confocal microscopy (Lens 40X). Nuclei were stained with DAPI (blue). Scale bars: 50 μ m. BV2 cells cultured in normoxia were used as negative control. Images are representative of three separate experiments.

3.3.2. Myricetin counteracts STAT1 phosphorylation induced by hypoxia in BV2 cells

In order to determine if Myr inhibits the hypoxia induced STAT1 phosphorylation, BV2 cells were pretreated with 50 μ M Myr for 30 min and, thereafter, cells were exposed to 1% O₂ for different times. The derived protein extracts were analyzed by Western Blot using specific antibody to identify Tyr701 phosphorylated STAT1. As shown in figure 32, the pretreatment with 50 μ M Myr inhibits STAT1 Tyr-phosphorylation under hypoxia. Myr treatments do not alter the total levels of STAT1 protein.

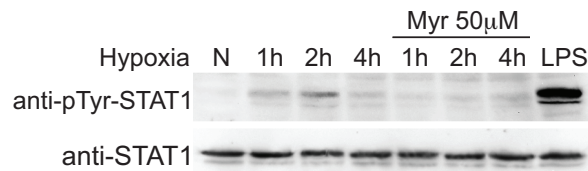


Figure 32. Myr counteracts hypoxia-induced STAT1 Tyr-phosphorylation in BV2 cells. BV2 cells were pretreated or not with 50 μ M Myr for 30 min and, thereafter, exposed to hypoxia for 1,2 or 4 hours. The whole protein extracts were analyzed by Western Blot using anti-phosphoTyr701-STAT1 antibody. The protein extract from BV2 cells cultured under normoxia was used as negative control (N). Treatment with 100ng/mL LPS was used as positive control. Images are representative of four separate experiments.

The analysis by confocal microscopy confirmed that Myr treatment inhibits tyrosine phosphorylation of STAT1 switching off this signal (Fig.33).

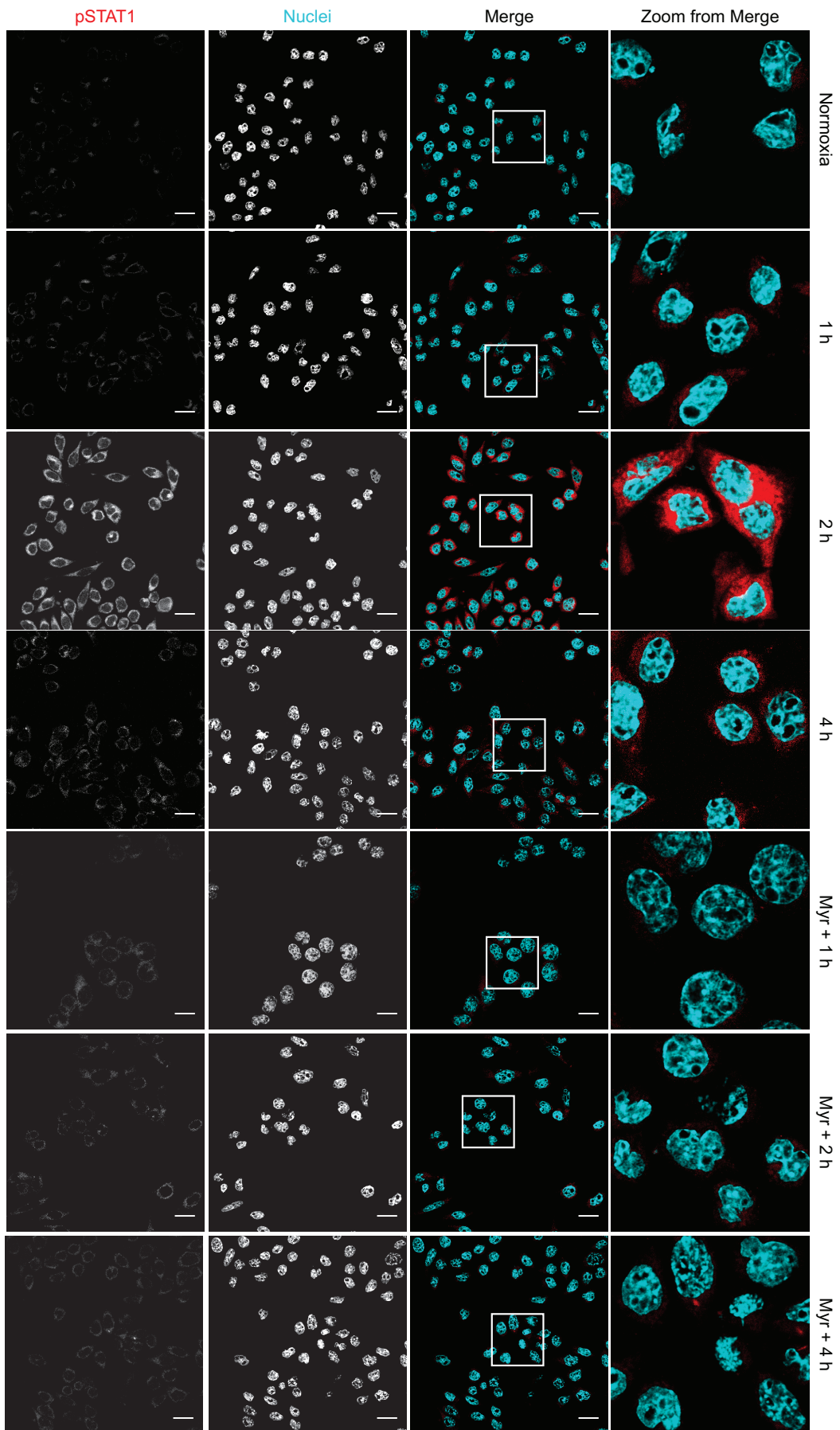


Figure 33. Myr counteracts hypoxia-induced STAT1 Tyr-phosphorylation in BV2 cells. BV2 cells, pretreated with 50 μ M Myr or not, were cultured under 1%O₂ for the indicated time. The cells were immunostained with phosphoTyr701-STAT1 antibody (red) and analyzed by confocal microscopy (Lens 40X). Nuclei were stained with DAPI (blue). Scale bars: 50 μ m. Images are representative for three separate experiments.

3.3.3. Myricetin prevents SH-SY5Y cells death induced by hypoxia-activated BV2 cells

The effect of Myr in preventing neuronal death induced by M1 activated microglia was evaluated in the cross-talk *in vitro* cellular model. BV2 cells, pretreated or not with 50 μ M Myr for 30 min, were activated under hypoxia for 24 hours. The conditioned medium of these cells (Myr+H-BV2-CM; H-BV2-CM) were used to culture SH-SY5Y cells under hypoxia for 24 hours. SH-SY5Y treated with N-BV2-CM was used as control. As shown in figure 34, the viability of SH-SY5Y cells treated with H-BV2-CM was 54.33 \pm 1.45% whereas that of cells treated with Myr+H-BV2-CM was 66.67 \pm 0.88%. The statistical analysis reveals that Myr+H-BV2-CM significantly prevents the SH-SY5Y cells death compared to H-BV2-CM. (*p<0.005). Myr treatment alone does not affect cells viability (Data not shown).

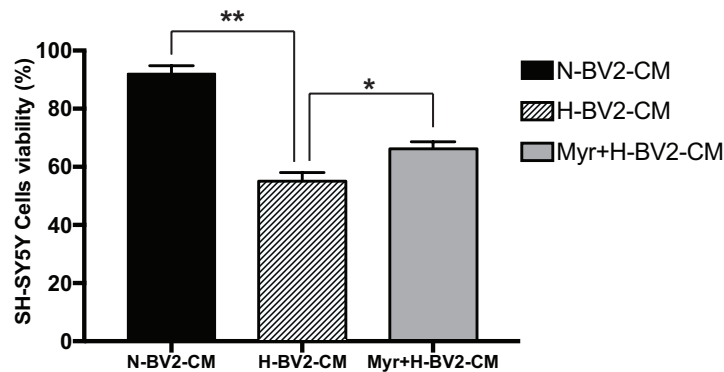


Figure 34. Myr prevents SH-SY5Y cells death induced by hypoxia-activated BV2 cells. The viability (%) of SH-SY5Y cells cultured under hypoxia for 24 hour in N-BV2-CM (■), H-BV2-CM (▨) and Myr+H-BV2-CM (■) are shown. Treatment with Myr+H-BV2-CM partially prevents SH-SY5Y cells death compared to H-BV2-CM treatment. Values represent the mean \pm SEM of three separate experiments. *p<0.005.

Altogether, the present data indicate the ability of Myr to inhibit hypoxia-induced tyrosine phosphorylation of STAT1 preventing the consequent microglia activation.

4. Discussion

The ubiquitous transcriptional factor STAT1 activates the expression of important genes involved in inflammatory and in apoptotic processes, transducing the signal of several pro-inflammatory cytokines and growth factors from the outer of the cell to the nucleus. It is known that the signaling cascade of STAT1 is hyper-activated in pathologies related to acute (e.g. cardiac or cerebral ischemia/reperfusion damage or angina pectoris) or chronic inflammation (e.g. asthma, rheumatoid arthritis, Chron's or Alzheimer's diseases). During the past 10 years, it has been demonstrated that the inflammatory process is strictly correlated to oxidative stress that triggers and exacerbates the inflammatory response through the modulation of several intracellular signaling pathways. In this context, it has been reported that H₂O₂, induces tyrosine phosphorylation of STAT1 and activates STAT1 signaling in different glia cells contributing to the development and progression of neurodegenerative diseases XX). Some authors correlate this ability of H₂O₂ to an increase in tyrosine kinase activity. Recently, the research group in which I performed my PhD thesis, proved that H₂O₂ treatment induces reversible S-glutathionylation of recombinant purified form of STAT1 pointing out at molecular level how oxidative stress hyper-activates STAT1. Moreover, by mass spectrometry strategies they identify two cysteine residue, Cys324 and Cys492, as the main targets of S-glutathionylation [148]. The computer modelling analysis of crystal structure of STAT1 (PDB: 1BF5) reveals that the Cys324 is located in the DBD domain while the Cys492 is between the DBD and the LD domains within STAT1 sequence and both the residues are particularly exposed to the solvent, one of the major requirements for protein S-glutathionylation (Fig. 35)

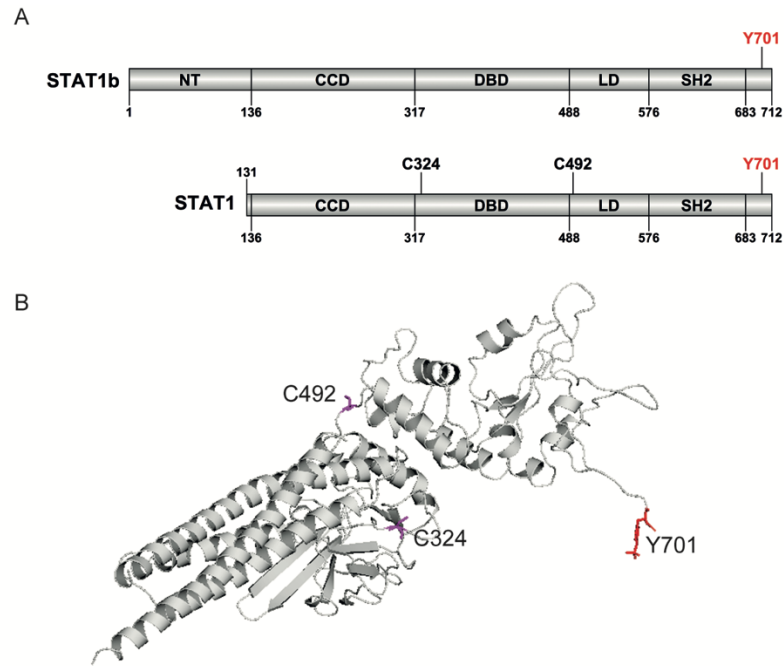


Figure 35. Identification of the cysteine residues involved in STAT1 S-glutathionylation. A) Cys324 and Cys492 within the structure scheme of STAT1 functional domains. B) Cys324 and Cys492 within the crystal structure 1BF5 of STAT1. doi: 10.1016/j.freeradbiomed.2018.02.005

To shed light on redox regulation of STAT1 in cells, we analysed the effect of physiological oxidant stimuli on STAT1 activation using microglia BV2 cell line. Herein we demonstrate that H₂O₂ as well as hypoxia treatments rapidly induces S-glutathionylation of STAT1. Modified STAT1 was rapidly phosphorylated, and was able to bind a specific DNA consensus sequence for STAT1. The reversibility of the modification was confirmed by treating the BV2 cells with the DTT, a disulfide reducing agent. These data indicate that S-thiolation of STAT1 does not impair either phosphorylation or translocation into the nucleus, suggesting a putative regulatory role for this modification. The involvement of Cys324 and Cys492 in the redox regulation of STAT1 in cells was evaluated transfecting STAT1-null BV2 cells with site-specific mutants. These proteins were generated substituting one or two cysteine residues with serine that should retain the approximate size, geometry, and polarity of the cysteine residues but would be unable to form disulphide bonds. Only the C324/492S double mutant, is resistant to glutathionylation, phosphorylation and is not able to bind DNA consensus sequence of STAT1 in transfected in STAT1-null BV2 cells under oxidative stress. These data confirm the regulatory function of this modification

and the critical role of the identified residues in the redox regulation of STAT1. It is important to note that C324S mutant was less phosphorylated respect to WT STAT1 under oxidative stress suggesting the key role of this residue in the activation of STAT1 transcription pathway.

Recently, S-glutathionylation has been reported to act as a signaling mechanism in physiological and pathological conditions. Indeed, despite being a protective mechanism against thiol irreversible oxidation, this post-translational modification can also regulate protein function under alteration of redox homeostasis. Nowadays, it is known that cerebral hypoxia is closely associated with the onset and progression of chronic neuroinflammation in pathological conditions such as Alzheimer's, Parkinson's and Huntington's diseases, amyotrophic lateral sclerosis and cerebrovascular diseases [154]–[157]. Moreover, it has been reported that the oxidative stress derived from hypoxic condition leads to M1 activation in primary rat microglia as well as in in vivo model of brain ischemia [158]. Consistently with earlier publications, the typical morphology of M1 microglia phenotype has been observed in BV2 cells after 1 hour of exposure to 1% O₂. The murine microglia cells showed increased expression of pro-inflammatory factors iNOS and COX2 and of the M1 marker CD68 starting from 18 hours of exposure to hypoxia. In addition, it has been observed that pre-treating BV2 cells with NAC, which acts as ROS scavenger and preserve the GSH levels, or with GEE, that re-establish the GSH content within the cells, counteract M1 polarization induced by hypoxia. Although several reports examined M1 microglia activation triggered by hypoxia, the molecular mechanism has not been clarified yet. It has been demonstrated that several signaling molecules and transcription factors, including HIF-1 α , NF- κ B and STAT1, are modulated in activated microglia during brain ischemia [159]–[161]. In microglia cells, NF- κ B is involved in the up-regulation of pro-inflammatory molecules release (e.g. TNF- α and IL-1 β) and in neuronal damage induced by brain ischemia [162], [163]. Furthermore, the activation of STAT1 pathway is involved in classical M1 polarization after IFN- γ or LPS exposure and it has been reported that it plays a crucial role in the onset of ischemic brain injury in mice [118], [164]. To date, the role of STAT1 in microglia cells activation under hypoxia has not been investigated yet. Altogether our results demonstrate the

molecular mechanism of STAT1 signaling activation in BV2 cells under hypoxia pointing out the key role of S-glutathionylation of STAT1 in M1 microglia polarization.

Since STAT1 regulates both inflammatory response as well as apoptotic death, our findings on the redox regulation of STAT1 in activated microglia constitute the bases for further study on STAT1 as mediator of neuronal death during neuroinflammation. In this context, it could be interesting to investigate if phytochemical compounds with anti-STAT1 activity have the ability to counteract microglia activation in order to develop an adjuvant therapy. It is known that myricetin exhibit a strong and specific anti-STAT1 activity, besides the antioxidant effect typical of polyphenolic compounds. This effect is strictly related to their molecular structure that allows the direct interaction with critical sites near the SH2 domain of STAT1 protein with high affinity preventing the phosphorylation of the transcription factor [153].

To deep inside this aspect, we set up a cross-talk model between microglia and neurons in hypoxic environment. We demonstrate that conditioned media from BV2 cells activated under hypoxia for 24 hours induce a significant increase in SH-SY5Y cells death after 24h of treatment. The analysis of apoptosis hallmarks such as Annexin-V exposure on cell membrane and PARP cleavage in SH-SY5Y cells confirm this as the mechanism of neuronal death induced by hypoxia-activated microglia. Thereafter, the ability of myricetin to counteract the M1 microglia activation induced by hypoxia has been tested. As expected myricetin pretreatment was able to counteract STAT1 tyrosine phosphorylation and prevent M1 microglia polarization in BV2 cells cultured under hypoxia. Intriguingly, myricetin significantly protects SH-SY5Y cells from apoptosis induced by activated microglia in the cross-talk cellular model. These results could be also a starting point for further tests on other phytochemical-derived molecules that selectively inhibit STAT1 signaling to treat neuroinflammatory diseases in which this transcriptional factor plays a key role.

In conclusion, the present study demonstrates that the transcriptional factor STAT1 is a redox sensitive protein and that S-glutathionylation may be the mechanism through which it is activated under oxidative stress. Finally, the data prove that the natural flavonoid myricetin is able to counteract pro-inflammatory microglia activation thanks to its highly specific anti-STAT1 activity.

5. Bibliography

- [1] J. E. Darnell, “STATs and gene regulation,” *Science*, vol. 277, no. 5332, pp. 1630–1635, Sep. 1997.
- [2] C. I. Santos and A. P. Costa-Pereira, “Signal transducers and activators of transcription—from cytokine signalling to cancer biology,” *Biochim. Biophys. Acta*, vol. 1816, no. 1, pp. 38–49, Aug. 2011.
- [3] J. E. Darnell, I. M. Kerr, and G. R. Stark, “Jak-STAT pathways and transcriptional activation in response to IFNs and other extracellular signaling proteins,” *Science*, vol. 264, no. 5164, pp. 1415–1421, Jun. 1994.
- [4] A. H. Brivanlou and J. E. Darnell, “Signal transduction and the control of gene expression,” *Science*, vol. 295, no. 5556, pp. 813–818, Feb. 2002.
- [5] K. Schroder, P. J. Hertzog, T. Ravasi, and D. A. Hume, “Interferon-gamma: an overview of signals, mechanisms and functions,” *J. Leukoc. Biol.*, vol. 75, no. 2, pp. 163–189, Feb. 2004.
- [6] C. V. Ramana, M. Chatterjee-Kishore, H. Nguyen, and G. R. Stark, “Complex roles of Stat1 in regulating gene expression,” *Oncogene*, vol. 19, no. 21, pp. 2619–2627, May 2000.
- [7] Y. Jiang et al., “STAT1 mediates transmembrane TNF-alpha-induced formation of death-inducing signaling complex and apoptotic signaling via TNFR1,” *Cell Death Differ.*, vol. 24, no. 4, pp. 660–671, 2017.
- [8] H. S. Kim and M.-S. Lee, “STAT1 as a key modulator of cell death,” *Cell. Signal.*, vol. 19, no. 3, pp. 454–465, Mar. 2007.
- [9] A. Stephanou et al., “Ischemia-induced STAT-1 expression and activation play a critical role in cardiomyocyte apoptosis,” *J. Biol. Chem.*, vol. 275, no. 14, pp. 10002–10008, Apr. 2000.
- [10] Y. Wang et al., “Autophagy regulates inflammation following oxidative injury in diabetes,” *Autophagy*, vol. 9, no. 3, pp. 272–277, Mar. 2013.
- [11] A. Martí-Rodrigo et al., “Rilpivirine attenuates liver fibrosis through selective STAT1-mediated apoptosis in hepatic stellate cells,” *Gut*, Sep. 2019.
- [12] A. Piaszyk-Borychowska et al., “Signal Integration of IFN-I and IFN-II With TLR4 Involves Sequential Recruitment of STAT1-Complexes and NFκB to Enhance Pro-inflammatory Transcription,” *Front. Immunol.*, vol. 10, p. 1253, 2019.
- [13] T. S. Lin, S. Mahajan, and D. A. Frank, “STAT signaling in the pathogenesis and treatment of leukemias,” *Oncogene*, vol. 19, no. 21, pp. 2496–2504, May 2000.

- [14] L. Martinez-Martinez et al., "A novel gain-of-function STAT1 mutation resulting in basal phosphorylation of STAT1 and increased distal IFN- γ -mediated responses in chronic mucocutaneous candidiasis," *Mol. Immunol.*, vol. 68, no. 2 Pt C, pp. 597–605, Dec. 2015.
- [15] G. Giardino et al., "Novel STAT1 gain-of-function mutation and suppurative infections," *Pediatr. Allergy Immunol. Off. Publ. Eur. Soc. Pediatr. Allergy Immunol.*, vol. 27, no. 2, pp. 220–223, Mar. 2016.
- [16] X. Chen, U. Vinkemeier, Y. Zhao, D. Jeruzalmi, J. E. Darnell, and J. Kuriyan, "Crystal structure of a tyrosine phosphorylated STAT-1 dimer bound to DNA," *Cell*, vol. 93, no. 5, pp. 827–839, May 1998.
- [17] H. S. Kim and M.-S. Lee, "STAT1 as a key modulator of cell death," *Cell. Signal.*, vol. 19, no. 3, pp. 454–465, Mar. 2007.
- [18] A. Marg, Y. Shan, T. Meyer, T. Meissner, M. Brandenburg, and U. Vinkemeier, "Nucleocytoplasmic shuttling by nucleoporins Nup153 and Nup214 and CRM1-dependent nuclear export control the subcellular distribution of latent Stat1," *J. Cell Biol.*, vol. 165, no. 6, pp. 823–833, Jun. 2004.
- [19] A. Stephanou and D. S. Latchman, "Opposing actions of STAT-1 and STAT-3," *Growth Factors Chur Switz.*, vol. 23, no. 3, pp. 177–182, Sep. 2005.
- [20] Z. Wen, Z. Zhong, and J. E. Darnell, "Maximal activation of transcription by Stat1 and Stat3 requires both tyrosine and serine phosphorylation," *Cell*, vol. 82, no. 2, pp. 241–250, Jul. 1995.
- [21] T. Decker and P. Kovarik, "Serine phosphorylation of STATs," *Oncogene*, vol. 19, no. 21, pp. 2628–2637, May 2000.
- [22] D. E. Levy and J. E. Darnell, "Stats: transcriptional control and biological impact," *Nat. Rev. Mol. Cell Biol.*, vol. 3, no. 9, pp. 651–662, Sep. 2002.
- [23] M. Parrini et al., "The C-Terminal Transactivation Domain of STAT1 Has a Gene-Specific Role in Transactivation and Cofactor Recruitment," *Front. Immunol.*, vol. 9, p. 2879, 2018.
- [24] U. Vinkemeier, S. L. Cohen, I. Moarefi, B. T. Chait, J. Kuriyan, and J. E. Darnell, "DNA binding of in vitro activated Stat1 alpha, Stat1 beta and truncated Stat1: interaction between NH2-terminal domains stabilizes binding of two dimers to tandem DNA sites," *EMBO J.*, vol. 15, no. 20, pp. 5616–5626, Oct. 1996.
- [25] Q. Ning et al., "STAT1 and STAT3 alpha/beta splice form activation predicts host responses in mouse hepatitis virus type 3 infection," *J. Med. Virol.*, vol. 69, no. 3, pp. 306–312, Mar. 2003.

- [26] F. Baran-Marszak et al., “Differential roles of STAT1alpha and STAT1beta in fludarabine-induced cell cycle arrest and apoptosis in human B cells,” *Blood*, vol. 104, no. 8, pp. 2475–2483, Oct. 2004.
- [27] G. R. Stark, I. M. Kerr, B. R. Williams, R. H. Silverman, and R. D. Schreiber, “How cells respond to interferons,” *Annu. Rev. Biochem.*, vol. 67, pp. 227–264, 1998.
- [28] J. J. O’Shea, “Jaks, STATs, cytokine signal transduction, and immunoregulation: are we there yet?,” *Immunity*, vol. 7, no. 1, pp. 1–11, Jul. 1997.
- [29] T. Kisseleva, S. Bhattacharya, J. Braunstein, and C. W. Schindler, “Signaling through the JAK/STAT pathway, recent advances and future challenges,” *Gene*, vol. 285, no. 1–2, pp. 1–24, Feb. 2002.
- [30] K. Igarashi et al., “Interferon-gamma induces tyrosine phosphorylation of interferon-gamma receptor and regulated association of protein tyrosine kinases, Jak1 and Jak2, with its receptor,” *J. Biol. Chem.*, vol. 269, no. 20, pp. 14333–14336, May 1994.
- [31] K. M. McBride and N. C. Reich, “The ins and outs of STAT1 nuclear transport,” *Sci. STKE Signal Transduct. Knowl. Environ.*, vol. 2003, no. 195, p. RE13, Aug. 2003.
- [32] Y. M. Chook and G. Blobel, “Karyopherins and nuclear import,” *Curr. Opin. Struct. Biol.*, vol. 11, no. 6, pp. 703–715, Dec. 2001.
- [33] B. B. Hülsmann, A. A. Labokha, and D. Görlich, “The permeability of reconstituted nuclear pores provides direct evidence for the selective phase model,” *Cell*, vol. 150, no. 4, pp. 738–751, Aug. 2012.
- [34] R. Peters, “Translocation through the nuclear pore complex: selectivity and speed by reduction-of-dimensionality,” *Traffic Cph. Den.*, vol. 6, no. 5, pp. 421–427, May 2005.
- [35] K. M. McBride, G. Banninger, C. McDonald, and N. C. Reich, “Regulated nuclear import of the STAT1 transcription factor by direct binding of importin-alpha,” *EMBO J.*, vol. 21, no. 7, pp. 1754–1763, Apr. 2002.
- [36] R. Fagerlund, K. Mélen, L. Kinnunen, and I. Julkunen, “Arginine/lysine-rich nuclear localization signals mediate interactions between dimeric STATs and importin alpha 5,” *J. Biol. Chem.*, vol. 277, no. 33, pp. 30072–30078, Aug. 2002.
- [37] T. Sekimoto, N. Imamoto, K. Nakajima, T. Hirano, and Y. Yoneda, “Extracellular signal-dependent nuclear import of Stat1 is mediated by nuclear pore-targeting complex formation with NPI-1, but not Rch1,” *EMBO J.*, vol. 16, no. 23, pp. 7067–7077, Dec. 1997.
- [38] T. Sekimoto, K. Nakajima, T. Tachibana, T. Hirano, and Y. Yoneda, “Interferon-gamma-dependent nuclear import of Stat1 is mediated by the GTPase activity of Ran/TC4,” *J. Biol. Chem.*, vol. 271, no. 49, pp. 31017–31020, Dec. 1996.

- [39] J. J. Rodriguez, C. D. Cruz, and C. M. Horvath, "Identification of the nuclear export signal and STAT-binding domains of the Nipah virus V protein reveals mechanisms underlying interferon evasion," *J. Virol.*, vol. 78, no. 10, pp. 5358–5367, May 2004.
- [40] K. M. McBride, C. McDonald, and N. C. Reich, "Nuclear export signal located within the DNA-binding domain of the STAT1 transcription factor," *EMBO J.*, vol. 19, no. 22, pp. 6196–6206, Nov. 2000.
- [41] K. Shuai and B. Liu, "Regulation of JAK-STAT signalling in the immune system," *Nat. Rev. Immunol.*, vol. 3, no. 11, pp. 900–911, Nov. 2003.
- [42] T. R. Wu et al., "SHP-2 is a dual-specificity phosphatase involved in Stat1 dephosphorylation at both tyrosine and serine residues in nuclei," *J. Biol. Chem.*, vol. 277, no. 49, pp. 47572–47580, Dec. 2002.
- [43] J. ten Hoeve et al., "Identification of a nuclear Stat1 protein tyrosine phosphatase," *Mol. Cell. Biol.*, vol. 22, no. 16, pp. 5662–5668, Aug. 2002.
- [44] S. E. Nicholson et al., "Mutational analyses of the SOCS proteins suggest a dual domain requirement but distinct mechanisms for inhibition of LIF and IL-6 signal transduction," *EMBO J.*, vol. 18, no. 2, pp. 375–385, Jan. 1999.
- [45] A. Matsumoto et al., "CIS, a cytokine inducible SH2 protein, is a target of the JAK-STAT5 pathway and modulates STAT5 activation," *Blood*, vol. 89, no. 9, pp. 3148–3154, May 1997.
- [46] F. Verdier et al., "Proteasomes regulate erythropoietin receptor and signal transducer and activator of transcription 5 (STAT5) activation. Possible involvement of the ubiquitinated Cis protein," *J. Biol. Chem.*, vol. 273, no. 43, pp. 28185–28190, Oct. 1998.
- [47] K. Shuai, "Modulation of STAT signaling by STAT-interacting proteins," *Oncogene*, vol. 19, no. 21, pp. 2638–2644, May 2000.
- [48] B. Liu et al., "Inhibition of Stat1-mediated gene activation by PIAS1," *Proc. Natl. Acad. Sci. U. S. A.*, vol. 95, no. 18, pp. 10626–10631, Sep. 1998.
- [49] J. Long, I. Matsuura, D. He, G. Wang, K. Shuai, and F. Liu, "Repression of Smad transcriptional activity by PIASy, an inhibitor of activated STAT," *Proc. Natl. Acad. Sci. U. S. A.*, vol. 100, no. 17, pp. 9791–9796, Aug. 2003.
- [50] R. S. Rogers, C. M. Horvath, and M. J. Matunis, "SUMO modification of STAT1 and its role in PIAS-mediated inhibition of gene activation," *J. Biol. Chem.*, vol. 278, no. 32, pp. 30091–30097, Aug. 2003.
- [51] H. Cheon, J. Yang, and G. R. Stark, "The functions of signal transducers and activators of transcription 1 and 3 as cytokine-inducible proteins," *J. Interferon Cytokine Res. Off. J. Int. Soc. Interferon Cytokine Res.*, vol. 31, no. 1, pp. 33–40, Jan. 2011.

- [52] H. Cheon and G. R. Stark, "Unphosphorylated STAT1 prolongs the expression of interferon-induced immune regulatory genes," *Proc. Natl. Acad. Sci. U. S. A.*, vol. 106, no. 23, pp. 9373–9378, Jun. 2009.
- [53] X. Mao et al., "Structural bases of unphosphorylated STAT1 association and receptor binding," *Mol. Cell*, vol. 17, no. 6, pp. 761–771, Mar. 2005.
- [54] Y. Zhang, Y. Chen, Z. Liu, and R. Lai, "ERK is a negative feedback regulator for IFN- γ /STAT1 signaling by promoting STAT1 ubiquitination," *BMC Cancer*, vol. 18, no. 1, p. 613, May 2018.
- [55] O. H. Krämer et al., "Acetylation of Stat1 modulates NF-kappaB activity," *Genes Dev.*, vol. 20, no. 4, pp. 473–485, Feb. 2006.
- [56] K. A. Mowen et al., "Arginine methylation of STAT1 modulates IFNalpha/beta-induced transcription," *Cell*, vol. 104, no. 5, pp. 731–741, Mar. 2001.
- [57] L. Altschuler, J. O. Wook, D. Gurari, J. Chebath, and M. Revel, "Involvement of receptor-bound protein methyltransferase PRMT1 in antiviral and antiproliferative effects of type I interferons," *J. Interferon Cytokine Res. Off. J. Int. Soc. Interferon Cytokine Res.*, vol. 19, no. 2, pp. 189–195, Feb. 1999.
- [58] C. Abramovich, B. Yakobson, J. Chebath, and M. Revel, "A protein-arginine methyltransferase binds to the intracytoplasmic domain of the IFNAR1 chain in the type I interferon receptor," *EMBO J.*, vol. 16, no. 2, pp. 260–266, Jan. 1997.
- [59] "Protein ISGylation modulates the JAK-STAT signaling pathway. - PubMed - NCBI." [Online].
Available: <https://www.ncbi.nlm.nih.gov/pubmed/12600939?dopt=Abstract>.
[Accessed: 04-Dec-2019].
- [60] M. Valko, D. Leibfritz, J. Moncol, M. T. D. Cronin, M. Mazur, and J. Telser, "Free radicals and antioxidants in normal physiological functions and human disease," *Int. J. Biochem. Cell Biol.*, vol. 39, no. 1, pp. 44–84, 2007.
- [61] P. D. Ray, B.-W. Huang, and Y. Tsuji, "Reactive oxygen species (ROS) homeostasis and redox regulation in cellular signaling," *Cell. Signal.*, vol. 24, no. 5, pp. 981–990, May 2012.
- [62] D. Giustarini, I. Dalle-Donne, D. Tsikas, and R. Rossi, "Oxidative stress and human diseases: Origin, link, measurement, mechanisms, and biomarkers," *Crit. Rev. Clin. Lab. Sci.*, vol. 46, no. 5–6, pp. 241–281, 2009.
- [63] V. Conti et al., "Antioxidant Supplementation in the Treatment of Aging-Associated Diseases," *Front. Pharmacol.*, vol. 7, p. 24, 2016.
- [64] C. P. Domingueti, L. M. S. Dusse, M. das G. Carvalho, L. P. de Sousa, K. B. Gomes, and A. P. Fernandes, "Diabetes mellitus: The linkage between oxidative stress,

- inflammation, hypercoagulability and vascular complications,” *J. Diabetes Complications*, vol. 30, no. 4, pp. 738–745, Jun. 2016.
- [65] V. Rani, G. Deep, R. K. Singh, K. Palle, and U. C. S. Yadav, “Oxidative stress and metabolic disorders: Pathogenesis and therapeutic strategies,” *Life Sci.*, vol. 148, pp. 183–193, Mar. 2016.
- [66] F. M. Aldakheel, P. S. Thomas, J. E. Bourke, M. C. Matheson, S. C. Dharmage, and A. J. Lowe, “Relationships between adult asthma and oxidative stress markers and pH in exhaled breath condensate: a systematic review,” *Allergy*, vol. 71, no. 6, pp. 741–757, 2016.
- [67] P. Lepetsos and A. G. Papavassiliou, “ROS/oxidative stress signaling in osteoarthritis,” *Biochim. Biophys. Acta*, vol. 1862, no. 4, pp. 576–591, 2016.
- [68] L. He, T. He, S. Farrar, L. Ji, T. Liu, and X. Ma, “Antioxidants Maintain Cellular Redox Homeostasis by Elimination of Reactive Oxygen Species,” *Cell. Physiol. Biochem. Int. J. Exp. Cell. Physiol. Biochem. Pharmacol.*, vol. 44, no. 2, pp. 532–553, 2017.
- [69] F. Q. Schafer and G. R. Buettner, “Redox environment of the cell as viewed through the redox state of the glutathione disulfide/glutathione couple,” *Free Radic. Biol. Med.*, vol. 30, no. 11, pp. 1191–1212, Jun. 2001.
- [70] D. S. Bilan, A. G. Shokhina, S. A. Lukyanov, and V. V. Belousov, “[Main Cellular Redox Couples],” *Bioorg. Khim.*, vol. 41, no. 4, pp. 385–402, Aug. 2015.
- [71] D. P. Jones and Y.-M. Go, “Redox compartmentalization and cellular stress,” *Diabetes Obes. Metab.*, vol. 12 Suppl 2, pp. 116–125, Oct. 2010.
- [72] S. C. Lu, “Glutathione synthesis,” *Biochim. Biophys. Acta*, vol. 1830, no. 5, pp. 3143–3153, May 2013.
- [73] D. P. Jones, “Redefining oxidative stress,” *Antioxid. Redox Signal.*, vol. 8, no. 9–10, pp. 1865–1879, Oct. 2006.
- [74] D. P. Jones and Y.-M. Go, “Redox compartmentalization and cellular stress,” *Diabetes Obes. Metab.*, vol. 12 Suppl 2, pp. 116–125, Oct. 2010.
- [75] Y.-M. Go and D. P. Jones, “Redox compartmentalization in eukaryotic cells,” *Biochim. Biophys. Acta*, vol. 1780, no. 11, pp. 1273–1290, Nov. 2008.
- [76] L. Flohé, “The fairytale of the GSSG/GSH redox potential,” *Biochim. Biophys. Acta*, vol. 1830, no. 5, pp. 3139–3142, May 2013.
- [77] A. Pastore, G. Federici, E. Bertini, and F. Piemonte, “Analysis of glutathione: implication in redox and detoxification,” *Clin. Chim. Acta Int. J. Clin. Chem.*, vol. 333, no. 1, pp. 19–39, Jul. 2003.
- [78] O. W. Griffith, “Biologic and pharmacologic regulation of mammalian glutathione synthesis,” *Free Radic. Biol. Med.*, vol. 27, no. 9–10, pp. 922–935, Nov. 1999.

- [79] D. P. Jones, "Redox sensing: orthogonal control in cell cycle and apoptosis signalling," *J. Intern. Med.*, vol. 268, no. 5, pp. 432–448, Nov. 2010.
- [80] T. Finkel and N. J. Holbrook, "Oxidants, oxidative stress and the biology of ageing," *Nature*, vol. 408, no. 6809, pp. 239–247, Nov. 2000.
- [81] S. G. Rhee, Y. S. Bae, S. R. Lee, and J. Kwon, "Hydrogen peroxide: a key messenger that modulates protein phosphorylation through cysteine oxidation," *Sci. STKE Signal Transduct. Knowl. Environ.*, vol. 2000, no. 53, p. pe1, Oct. 2000.
- [82] M.-A. Sun, Q. Zhang, Y. Wang, W. Ge, and D. Guo, "Prediction of redox-sensitive cysteines using sequential distance and other sequence-based features," *BMC Bioinformatics*, vol. 17, no. 1, p. 316, Aug. 2016.
- [83] P. Ghezzi, "Regulation of protein function by glutathionylation," *Free Radic. Res.*, vol. 39, no. 6, pp. 573–580, Jun. 2005.
- [84] I. Dalle-Donne, R. Rossi, G. Colombo, D. Giustarini, and A. Milzani, "Protein S-glutathionylation: a regulatory device from bacteria to humans," *Trends Biochem. Sci.*, vol. 34, no. 2, pp. 85–96, Feb. 2009.
- [85] T. Adachi et al., "S-Glutathionylation by peroxynitrite activates SERCA during arterial relaxation by nitric oxide," *Nat. Med.*, vol. 10, no. 11, pp. 1200–1207, Nov. 2004.
- [86] A. J. Cooper, J. T. Pinto, and P. S. Callery, "Reversible and irreversible protein glutathionylation: biological and clinical aspects," *Expert Opin. Drug Metab. Toxicol.*, vol. 7, no. 7, pp. 891–910, Jul. 2011.
- [87] M. Fratelli et al., "Identification by redox proteomics of glutathionylated proteins in oxidatively stressed human T lymphocytes," *Proc. Natl. Acad. Sci. U. S. A.*, vol. 99, no. 6, pp. 3505–3510, Mar. 2002.
- [88] D. Giustarini, R. Rossi, A. Milzani, R. Colombo, and I. Dalle-Donne, "S-glutathionylation: from redox regulation of protein functions to human diseases," *J. Cell. Mol. Med.*, vol. 8, no. 2, pp. 201–212, Jun. 2004.
- [89] P. Klatt and S. Lamas, "Regulation of protein function by S-glutathionylation in response to oxidative and nitrosative stress," *Eur. J. Biochem.*, vol. 267, no. 16, pp. 4928–4944, Aug. 2000.
- [90] I. A. Cotgreave and R. G. Gerdes, "Recent trends in glutathione biochemistry--glutathione-protein interactions: a molecular link between oxidative stress and cell proliferation?," *Biochem. Biophys. Res. Commun.*, vol. 242, no. 1, pp. 1–9, Jan. 1998.
- [91] E. Butturini et al., "S-Glutathionylation at Cys328 and Cys542 impairs STAT3 phosphorylation," *ACS Chem. Biol.*, vol. 9, no. 8, pp. 1885–1893, Aug. 2014.

- [92] P. Klatt et al., “Redox regulation of c-Jun DNA binding by reversible S-glutathiolation,” *FASEB J. Off. Publ. Fed. Am. Soc. Exp. Biol.*, vol. 13, no. 12, pp. 1481–1490, Sep. 1999.
- [93] E. Pineda-Molina et al., “Glutathionylation of the p50 subunit of NF-kappaB: a mechanism for redox-induced inhibition of DNA binding,” *Biochemistry*, vol. 40, no. 47, pp. 14134–14142, Nov. 2001.
- [94] M. Lyman, D. G. Lloyd, X. Ji, M. P. Vizcaychipi, and D. Ma, “Neuroinflammation: the role and consequences,” *Neurosci. Res.*, vol. 79, pp. 1–12, Feb. 2014.
- [95] M. Schain and W. C. Kreisl, “Neuroinflammation in Neurodegenerative Disorders-a Review,” *Curr. Neurol. Neurosci. Rep.*, vol. 17, no. 3, p. 25, 2017.
- [96] T. Wyss-Coray and L. Mucke, “Inflammation in neurodegenerative disease--a double-edged sword,” *Neuron*, vol. 35, no. 3, pp. 419–432, Aug. 2002.
- [97] “Mitochondrial dysfunction and oxidative stress in neurodegenerative diseases. - PubMed - NCBI.” [Online]. Available: <https://www.ncbi.nlm.nih.gov/pubmed/?term=nature+443%3A787-795%3B+2006>. [Accessed: 04-Dec-2019].
- [98] R. E. Mrak and W. S. T. Griffin, “Glial cells and their cytokines in progression of neurodegeneration,” *Neurobiol. Aging*, vol. 26, no. 3, pp. 349–354, Mar. 2005.
- [99] L. C. Walker and H. LeVine, “The cerebral proteopathies: neurodegenerative disorders of protein conformation and assembly,” *Mol. Neurobiol.*, vol. 21, no. 1–2, pp. 83–95, Apr. 2000.
- [100] H. T. Orr and H. Y. Zoghbi, “Reversing neurodegeneration: a promise unfolds,” *Cell*, vol. 101, no. 1, pp. 1–4, Mar. 2000.
- [101] M. L. Block and J.-S. Hong, “Microglia and inflammation-mediated neurodegeneration: multiple triggers with a common mechanism,” *Prog. Neurobiol.*, vol. 76, no. 2, pp. 77–98, Jun. 2005.
- [102] W. M. Cowan and E. R. Kandel, “Prospects for neurology and psychiatry,” *JAMA*, vol. 285, no. 5, pp. 594–600, Feb. 2001.
- [103] G. W. Kreutzberg, “Microglia: a sensor for pathological events in the CNS,” *Trends Neurosci.*, vol. 19, no. 8, pp. 312–318, Aug. 1996.
- [104] J. P. O’Callaghan and K. Sriram, “Glial fibrillary acidic protein and related glial proteins as biomarkers of neurotoxicity,” *Expert Opin. Drug Saf.*, vol. 4, no. 3, pp. 433–442, May 2005.
- [105] M. Eddleston and L. Mucke, “Molecular profile of reactive astrocytes--implications for their role in neurologic disease,” *Neuroscience*, vol. 54, no. 1, pp. 15–36, May 1993.

- [106] A. Vernadakis, "Neuron-glia interrelations," *Int. Rev. Neurobiol.*, vol. 30, pp. 149–224, 1988.
- [107] M. Beyer, U. Gimsa, I. Y. Eyüpoglu, N. P. Hailer, and R. Nitsch, "Phagocytosis of neuronal or glial debris by microglial cells: upregulation of MHC class II expression and multinuclear giant cell formation in vitro," *Glia*, vol. 31, no. 3, pp. 262–266, Sep. 2000.
- [108] F. Aloisi, "The role of microglia and astrocytes in CNS immune surveillance and immunopathology," *Adv. Exp. Med. Biol.*, vol. 468, pp. 123–133, 1999.
- [109] E. Hansson and L. Rönnbäck, "Astrocytes in glutamate neurotransmission," *FASEB J. Off. Publ. Fed. Am. Soc. Exp. Biol.*, vol. 9, no. 5, pp. 343–350, Mar. 1995.
- [110] R. von Bernhardi, L. Eugenin-von Bernhardi, and J. Eugenin, "Microglial cell dysregulation in brain aging and neurodegeneration," *Front. Aging Neurosci.*, vol. 7, p. 124, 2015.
- [111] D. Boche, V. H. Perry, and J. a. R. Nicoll, "Review: activation patterns of microglia and their identification in the human brain," *Neuropathol. Appl. Neurobiol.*, vol. 39, no. 1, pp. 3–18, Feb. 2013.
- [112] R. Awada et al., "Autotaxin downregulates LPS-induced microglia activation and pro-inflammatory cytokines production," *J. Cell. Biochem.*, vol. 115, no. 12, pp. 2123–2132, Dec. 2014.
- [113] P. Garção, C. R. Oliveira, and P. Agostinho, "Comparative study of microglia activation induced by amyloid-beta and prion peptides: role in neurodegeneration," *J. Neurosci. Res.*, vol. 84, no. 1, pp. 182–193, Jul. 2006.
- [114] R. A. Taylor and L. H. Sansing, "Microglial responses after ischemic stroke and intracerebral hemorrhage," *Clin. Dev. Immunol.*, vol. 2013, p. 746068, 2013.
- [115] B. A. Stoica et al., "PARP-1 inhibition attenuates neuronal loss, microglia activation and neurological deficits after traumatic brain injury," *J. Neurotrauma*, vol. 31, no. 8, pp. 758–772, Apr. 2014.
- [116] J. Schapansky, J. D. Nardozi, and M. J. LaVoie, "The complex relationships between microglia, alpha-synuclein, and LRRK2 in Parkinson's disease," *Neuroscience*, vol. 302, pp. 74–88, Aug. 2015.
- [117] U.-K. Hanisch and H. Kettenmann, "Microglia: active sensor and versatile effector cells in the normal and pathologic brain," *Nat. Neurosci.*, vol. 10, no. 11, pp. 1387–1394, Nov. 2007.
- [118] R. Orihuela, C. A. McPherson, and G. J. Harry, "Microglial M1/M2 polarization and metabolic states," *Br. J. Pharmacol.*, vol. 173, no. 4, pp. 649–665, Feb. 2016.

- [119] M. B. Graeber, “Changing face of microglia,” *Science*, vol. 330, no. 6005, pp. 783–788, Nov. 2010.
- [120] S. Gordon and P. R. Taylor, “Monocyte and macrophage heterogeneity,” *Nat. Rev. Immunol.*, vol. 5, no. 12, pp. 953–964, Dec. 2005.
- [121] G. Y. Chen and G. Nuñez, “Sterile inflammation: sensing and reacting to damage,” *Nat. Rev. Immunol.*, vol. 10, no. 12, pp. 826–837, Dec. 2010.
- [122] R. Shechter and M. Schwartz, “CNS sterile injury: just another wound healing?,” *Trends Mol. Med.*, vol. 19, no. 3, pp. 135–143, Mar. 2013.
- [123] C. A. McPherson, B. A. Merrick, and G. J. Harry, “In vivo molecular markers for pro-inflammatory cytokine M1 stage and resident microglia in trimethyltin-induced hippocampal injury,” *Neurotox. Res.*, vol. 25, no. 1, pp. 45–56, Jan. 2014.
- [124] J. S. Henkel, D. R. Beers, W. Zhao, and S. H. Appel, “Microglia in ALS: the good, the bad, and the resting,” *J. Neuroimmune Pharmacol. Off. J. Soc. NeuroImmune Pharmacol.*, vol. 4, no. 4, pp. 389–398, Dec. 2009.
- [125] R. M. Ransohoff and V. H. Perry, “Microglial physiology: unique stimuli, specialized responses,” *Annu. Rev. Immunol.*, vol. 27, pp. 119–145, 2009.
- [126] C. A. Colton and D. M. Wilcock, “Assessing activation states in microglia,” *CNS Neurol. Disord. Drug Targets*, vol. 9, no. 2, pp. 174–191, Apr. 2010.
- [127] X. Hu et al., “Sensitization of IFN-gamma Jak-STAT signaling during macrophage activation,” *Nat. Immunol.*, vol. 3, no. 9, pp. 859–866, Sep. 2002.
- [128] A. Yao et al., “Programmed death 1 deficiency induces the polarization of macrophages/microglia to the M1 phenotype after spinal cord injury in mice,” *Neurother. J. Am. Soc. Exp. Neurother.*, vol. 11, no. 3, pp. 636–650, Jul. 2014.
- [129] H. J. Cho et al., “Constitutive JAK2/STAT1 activation regulates endogenous BACE1 expression in neurons,” *Biochem. Biophys. Res. Commun.*, vol. 386, no. 1, pp. 175–180, Aug. 2009.
- [130] N. Kaur, B. Lu, R. K. Monroe, S. M. Ward, and S. W. Halvorsen, “Inducers of oxidative stress block ciliary neurotrophic factor activation of Jak/STAT signaling in neurons,” *J. Neurochem.*, vol. 92, no. 6, pp. 1521–1530, Mar. 2005.
- [131] J. A. Kim et al., “Inhibitory effect of a 2,4-bis(4-hydroxyphenyl)-2-butenal diacetate on neuro-inflammatory reactions via inhibition of STAT1 and STAT3 activation in cultured astrocytes and microglial BV-2 cells,” *Neuropharmacology*, vol. 79, pp. 476–487, Apr. 2014.
- [132] A. I. Rojo et al., “Redox control of microglial function: molecular mechanisms and functional significance,” *Antioxid. Redox Signal.*, vol. 21, no. 12, pp. 1766–1801, Oct. 2014.

- [133] B. A. Durafour et al., “Comparison of polarization properties of human adult microglia and blood-derived macrophages,” *Glia*, vol. 60, no. 5, pp. 717–727, May 2012.
- [134] A. Nimmerjahn, F. Kirchhoff, and F. Helmchen, “Resting microglial cells are highly dynamic surveillants of brain parenchyma in vivo,” *Science*, vol. 308, no. 5726, pp. 1314–1318, May 2005.
- [135] R. Franco and D. Fernández-Suárez, “Alternatively activated microglia and macrophages in the central nervous system,” *Prog. Neurobiol.*, vol. 131, pp. 65–86, Aug. 2015.
- [136] M. Sanson, E. Distel, and E. A. Fisher, “HDL induces the expression of the M2 macrophage markers arginase 1 and Fizz-1 in a STAT6-dependent process,” *PloS One*, vol. 8, no. 8, p. e74676, 2013.
- [137] K. E. Sheldon, H. Shandilya, D. Kepka-Lenhart, M. Poljakovic, A. Ghosh, and S. M. Morris, “Shaping the murine macrophage phenotype: IL-4 and cyclic AMP synergistically activate the arginase I promoter,” *J. Immunol. Baltim. Md 1950*, vol. 191, no. 5, pp. 2290–2298, Sep. 2013.
- [138] F. O. Martinez, L. Helming, and S. Gordon, “Alternative activation of macrophages: an immunologic functional perspective,” *Annu. Rev. Immunol.*, vol. 27, pp. 451–483, 2009.
- [139] L. Du, Y. Zhang, Y. Chen, J. Zhu, Y. Yang, and H.-L. Zhang, “Role of Microglia in Neurological Disorders and Their Potentials as a Therapeutic Target,” *Mol. Neurobiol.*, vol. 54, no. 10, pp. 7567–7584, 2017.
- [140] M. T. Lin and M. F. Beal, “Mitochondrial dysfunction and oxidative stress in neurodegenerative diseases,” *Nature*, vol. 443, no. 7113, pp. 787–795, Oct. 2006.
- [141] M. L. Block and J.-S. Hong, “Microglia and inflammation-mediated neurodegeneration: multiple triggers with a common mechanism,” *Prog. Neurobiol.*, vol. 76, no. 2, pp. 77–98, Jun. 2005.
- [142] S. Ullevig, H. S. Kim, and R. Asmis, “S-glutathionylation in monocyte and macrophage (dys)function,” *Int. J. Mol. Sci.*, vol. 14, no. 8, pp. 15212–15232, Jul. 2013.
- [143] L. A. Ralat, M. Ren, A. B. Schilling, and W.-J. Tang, “Protective role of Cys-178 against the inactivation and oligomerization of human insulin-degrading enzyme by oxidation and nitrosylation,” *J. Biol. Chem.*, vol. 284, no. 49, pp. 34005–34018, Dec. 2009.
- [144] A. D. Reynolds et al., “Nitrated alpha-synuclein and microglial neuroregulatory activities,” *J. Neuroimmune Pharmacol. Off. J. Soc. NeuroImmune Pharmacol.*, vol. 3, no. 2, pp. 59–74, Jun. 2008.

- [145] E. Butturini, D. Boriero, A. Carcereri de Prati, and S. Mariotto, “Immunoprecipitation methods to identify S-glutathionylation in target proteins,” *MethodsX*, vol. 6, pp. 1992–1998, 2019.
- [146] K. G. Reddie and K. S. Carroll, “Expanding the functional diversity of proteins through cysteine oxidation,” *Curr. Opin. Chem. Biol.*, vol. 12, no. 6, pp. 746–754, Dec. 2008.
- [147] J. J. Mieyal, M. M. Gallogly, S. Qanungo, E. A. Sabens, and M. D. Shelton, “Molecular mechanisms and clinical implications of reversible protein S-glutathionylation,” *Antioxid. Redox Signal.*, vol. 10, no. 11, pp. 1941–1988, Nov. 2008.
- [148] E. Butturini et al., “S-glutathionylation exerts opposing roles in the regulation of STAT1 and STAT3 signaling in reactive microglia,” *Free Radic. Biol. Med.*, vol. 117, pp. 191–201, 2018.
- [149] C. Kaur, G. Rathnasamy, and E.-A. Ling, “Roles of activated microglia in hypoxia induced neuroinflammation in the developing brain and the retina,” *J. Neuroimmune Pharmacol. Off. J. Soc. NeuroImmune Pharmacol.*, vol. 8, no. 1, pp. 66–78, Mar. 2013.
- [150] S. Y. Park et al., “Hypoxia induces nitric oxide production in mouse microglia via p38 mitogen-activated protein kinase pathway,” *Brain Res. Mol. Brain Res.*, vol. 107, no. 1, pp. 9–16, Oct. 2002.
- [151] T. Shabab, R. Khanabdali, S. Z. Moghadamtousi, H. A. Kadir, and G. Mohan, “Neuroinflammation pathways: a general review,” *Int. J. Neurosci.*, vol. 127, no. 7, pp. 624–633, Jul. 2017.
- [152] D. K. Semwal, R. B. Semwal, S. Combrinck, and A. Viljoen, “Myricetin: A Dietary Molecule with Diverse Biological Activities,” *Nutrients*, vol. 8, no. 2, p. 90, Feb. 2016.
- [153] T. M. Scarabelli et al., “Targeting STAT1 by myricetin and delphinidin provides efficient protection of the heart from ischemia/reperfusion-induced injury,” *FEBS Lett.*, vol. 583, no. 3, pp. 531–541, Feb. 2009.
- [154] C. Lu, A. Talukder, N. M. Savage, N. Singh, and K. Liu, “JAK-STAT-mediated chronic inflammation impairs cytotoxic T lymphocyte activation to decrease anti-PD-1 immunotherapy efficacy in pancreatic cancer,” *Oncoimmunology*, vol. 6, no. 3, p. e1291106, 2017.
- [155] D. Langlais, L. B. Barreiro, and P. Gros, “The macrophage IRF8/IRF1 regulome is required for protection against infections and is associated with chronic inflammation,” *J. Exp. Med.*, vol. 213, no. 4, pp. 585–603, Apr. 2016.
- [156] A. C. de Prati et al., “STAT1 as a new molecular target of anti-inflammatory treatment,” *Curr. Med. Chem.*, vol. 12, no. 16, pp. 1819–1828, 2005.

- [157] A. Stephanou et al., "Ischemia-induced STAT-1 expression and activation play a critical role in cardiomyocyte apoptosis," *J. Biol. Chem.*, vol. 275, no. 14, pp. 10002–10008, Apr. 2000.
- [158] J. Boddaert et al., "CD8 signaling in microglia/macrophage M1 polarization in a rat model of cerebral ischemia," *PloS One*, vol. 13, no. 1, p. e0186937, 2018.
- [159] N. S. Kenneth and S. Rocha, "Regulation of gene expression by hypoxia," *Biochem. J.*, vol. 414, no. 1, pp. 19–29, Aug. 2008.
- [160] Q. Xu, C. Jiang, Y. Rong, C. Yang, Y. Liu, and K. Xu, "The effects of fludarabine on rat cerebral ischemia," *J. Mol. Neurosci. MN*, vol. 55, no. 2, pp. 289–296, Feb. 2015.
- [161] D.-Y. Lu, H.-C. Liou, C.-H. Tang, and W.-M. Fu, "Hypoxia-induced iNOS expression in microglia is regulated by the PI3-kinase/Akt/mTOR signaling pathway and activation of hypoxia inducible factor-1alpha," *Biochem. Pharmacol.*, vol. 72, no. 8, pp. 992–1000, Oct. 2006.
- [162] A. Nurmi et al., "Nuclear factor-kappaB contributes to infarction after permanent focal ischemia," *Stroke*, vol. 35, no. 4, pp. 987–991, Apr. 2004.
- [163] I. Glezer, A. R. Simard, and S. Rivest, "Neuroprotective role of the innate immune system by microglia," *Neuroscience*, vol. 147, no. 4, pp. 867–883, Jul. 2007.
- [164] P. Przanowski et al., "The signal transducers Stat1 and Stat3 and their novel target Jmjd3 drive the expression of inflammatory genes in microglia," *J. Mol. Med. Berl. Ger.*, vol. 92, no. 3, pp. 239–254, Mar. 2014.

6. Appendix

During my second year as PhD student enrolled in the Molecular Medicine Program, I've spent 9 months (January-October, 2018) working in Professor D.A. Butterfield's laboratory at the University of Kentucky as visiting research scholar. Over this period, I've had worked on the project "Oxidative stress underlies Chemotherapy Induced Cognitive Impairment (CICI)", funded by the National Cancer Institute of the NIH.

Abstract

Chemotherapy induced cognitive impairment (CICI) is now widely known as a complication of chemotherapy that affects a large number of cancer survivors. Almost half of the chemotherapeutic agents approved by US Food and Drug Administration (FDA) have been reported to cause oxidative stress inducing directly or indirectly increased levels of reactive oxygen species (ROS) and it is known that oxidative stress is one of the main etio-pathological factors that can directly lead to cognitive impairment in CICI. In the past years, Butterfield's research group showed how the administration of the commonly used anti-cancer drug doxorubicin, due to its ability to generate ROS by redox cycling of its quinone component in its structure, results in oxidation of plasma proteins, such as apolipoprotein A1 (ApoA1) leading to tumor necrosis factor-alpha (TNF α)-mediated oxidative stress in mice plasma and brain. In the past twenty years, a new generation of cancer drugs, called target therapy, was developed. The activity of this class of anticancer drugs activity is highly selective against cancer cells. It known that, as many of classic chemotherapeutic agents, the target drugs likewise generate ROS. Venetoclax, or ABT199, is a target drug of the family of Bcl-2 inhibitors and approved by FDA for the treatment of Chronic Lymphocytic Leukemia (CLL). In this study, the ability of Venetoclax to induce oxidative stress after acute (100mg/Kg) and chronic (100mg/Kg/d for 7 days) treatment in mice plasma brain was investigated. Using novel object recognition (NOR), the presence of cognitive deficits was verified after ABT199 acute and chronic treatment. From these results, Venetoclax, although associated with ROS production like doxorubicin and other classical anticancer drugs, does not increase the oxidative

stress markers in mice plasma and brain after 1 day or 7 days of treatment. The Novel Object Recognition (NOR) test does not show a significant cognitive impairment in mice after treatment with acute or chronic ABT199.

Introduction

Chemotherapy induced cognitive impairment (CICI), called also “chemobrain” or “chemofog” by patients, is a well-known condition investigated since the ‘90s, that affects up to 70% of cancer survivors, depending on the study. CICI symptoms are due to serious neurological executive and cognitive deficits, particularly regarding attention, concentration, memory and multitasking functions [165], [166]. Moreover, the symptoms can be long term and last for 5-10 years post-chemotherapy. The cognitive impairment is also associated with brain structural changes such as a decreased volume in hippocampus, determined by MRI, and altered white and grey matters [167], [168]. At present, the underlying mechanisms that lead to the onset of CICI remain poorly understood. The candidate mechanisms proposed include oxidative stress, immunoinflammatory cytokine dysregulation, blood-brain barrier (BBB) integrity loss, genetic deficits, DNA damage and telomere length, and reduced hormone levels [169]. It is interesting that CICI is often linked to chemotherapeutic drugs that induce ROS production and oxidative stress but that do not cross the BBB. Among them, for example, doxorubicin, methotrexate, carmustine and cyclophamide [170]. In particular, ROS are mediators for mitochondrial dysfunction which can cause injuries in tissues where the mitochondrial activity is higher, like heart and brain [171]–[173]. In the past years, Butterfield’s research group investigated about the mechanism through which doxorubicin, a chemotherapeutic drug largely used in treatment of several types of cancer, induced CICI and about the key role of the proinflammatory cytokine TNF α in this process. Doxorubicin is known to induce oxidative stress in brain tissue, even if it cannot cross the BBB [174]. Because of its quinone structure, doxorubicin, after i.p. injection, undergoes redox cycling producing high levels of free radicals in plasma. The oxidative stress generated leads to the oxidative modification of plasma proteins. In particular, the oxidation of apolipoprotein A1 (ApoA1), which plays a role in regulation of TNF α levels in plasma, leads to increased peripheral levels

of this cytokine [175]. TNF α crosses the BBB inducing oxidative stress in brain parenchyma [176], [177]. Furthermore, TNF α also mediates the respiration impairment in brain mitochondria. Indeed, it has been demonstrated that TNF α , through the activation of NF- κ B and of the downstream molecule, inducible nitric oxide synthase, iNOS, causes nitrosative stress and the subsequent Mn-Superoxide Dismutase (MnSOD) nitration, leading to the dysfunction of brain mitochondria activity [178]. The consequences of all these events are apoptotic neuronal death and brain tissue damage that Butterfield hypothesizes leads to the CICI condition. In the last two decades, research focused on a new generation of cancer treatments, called molecular targeted therapy. The targeted drugs, highly selective against cancers cells, are designed to target molecules involved in carcinogenesis and tumor growth. Targeted drugs reportedly induce ROS generation and oxidative stress [179]. However, if these drugs can cause CICI is still unknown. Among the targeted drug families, the Bcl-2 inhibitors act by increasing propensity of cancer cells for apoptosis [180]. Venetoclax, or ABT199, is a targeted drug belonging to the family of Bcl-2 inhibitors and approved by FDA for the treatment of Chronic Lymphocytic Leukemia (CLL) [181], [182]. Bcl-2 inhibitors, in addition to inhibiting their biochemical target, are associated with intracellular ROS generation that participates in their anticancer effects and they might be linked to the onset of CICI. I report here my investigation of whether ABT199 generates oxidative stress in plasma and in brain of mice and if such oxidative stress could potentially lead to the CICI condition.

Materials and methods

Reagents

All chemicals used throughout the present study were of the highest analytical grade, purchased from Sigma, unless otherwise specified.

Animal treatment

Wild type C57BL/6 mice, 12-13 weeks old, approximately 25-35g in size, were used. Two groups of mice, 10 males and 10 females, were used for ABT199 acute treatment (100mg/Kg); in each gender group 5 mice received vehicle (60% Phosal 50PG, 30% PEG 400, 10% ethanol) and 5 mice received drug. The same number of subjects was

used for ABT199 chronic treatment (100mg/Kg/d for 7 days). The drug or vehicle was administered through oral gavage using a 22 gauge stainless steel feed tube with rounded tip.

Behavioral test: Novel Object Recognition (NOR) test

The NOR test was performed starting 24h after ABT199 treatment. This behavioral test is used to evaluate cognition and recognition memory in rodent models of CNS disorders and it is based on the spontaneous tendency of rodents to explore a novel object rather than a familiar one [183]. The procedure provides three phases, to be performed in three consecutive days. Day 1: Habituation phase. During the first phase the mice were habituated to the testing room, for 1h, and to the empty arena (30cm x 30cm x 31.5cm) with no objects for 10 min for each single mouse. Day 2: Familiarization phase. During the second phase, after 30 min of habituation in the testing room, a single mouse was placed in the arena in presence of two identical objects for 10 min. Day 3: Testing phase. After 24h from the second phase, the mice were bring in the testing room 30 min before to start the test. In testing phase, each mouse explored the arena, where one of the objects was replaced with a novel one, for 10 min. During phases 2 and 3 mice were recorded and the time spent exploring each object was calculated. Data are reported as Discrimination Index (DI), which allows to highlight the discrimination between the novel and the familiar objects. A positive score indicates more time spent with the novel object, a negative score indicates a preference for the familiar object. The DI is calculated as $DI = (TN - TF) / (TN + TF)$; TN=time spent exploring the novel object, TF= time spent exploring the familiar object. All mice where sacrificed after the end of the NOR test and the tissue collected for the oxidative stress studies.

Plasma samples preparation

Mice were sacrificed 72h after treatment, following the NOR behavioral test. Whole blood was collected via cardiac puncture of the left ventricle with a 1cc syringe. Blood was transferred in EDTA-coated vials (BD) and centrifuged at 3000g for 10 min at 4°C. Plasma was collected and diluted 10-fold with PBS in presence of protease and phosphatase inhibitors (PMSF 0.2mM, Leupeptin 4µg/ml, Pepstatin 4µg/ml, Aprotinin 5µg/ml, Phosphatase inhibitors cocktail). The protein concentration was

assayed by the Pierce BCA method (Pierce™ BCA Protein Assay Kit. Thermo Fisher Scientific).

Brain tissue homogenization

Mice were sacrificed 72h after treatment, following the NOR behavioral test. Brains were isolated and homogenate in RIPA buffer (Tris-HCl 50mM, NaCl 150mM, NP40 1%, Sodium Deoxycholate 0.5%, SDS 0.1%, pH 8.0) in presence of protease and phosphatase inhibitors (PMSF 0.2mM, Leupeptin 4µg/ml, Pepstatin 4µg/ml, Aprotinin 5µg/ml, Phosphatase inhibitors cocktail) using a glass Potter. The homogenate was sonicated and centrifuged 14000g for 30 min at 4°C. The protein concentration was assayed by the Pierce BCA method.

Slot blot assays

The slot blot method was used to determine levels of protein carbonyls (PC), 3-nitrotyrosine (3-NT) and protein-bound to 4-hydroxynonenal (HNE) in mice plasma and brain. To determine protein carbonyl content, samples were derivatized with 2,4-dinitrophenylhydrazine (DNPH) using OxyBlot Protein Oxidation detection Kit (Millipore). For 3-NT and HNE samples were solubilized in Laemmli buffer (Tris-HCl 0.125M, 4% SDS, 20% glycerol, pH 6.8). Proteins from each samples were loaded on a nitrocellulose membrane (Bio-Rad) in a slot blot apparatus (Bio-Rad) under vacuum (250ng for PC from both plasma and brain; 250ng for 3-NT and HNE from brain; 500ng for 3-NT and HNE from plasma). Membranes were blocked in 3% bovine serum albumin (BSA) diluted in Tris-buffered saline with Tween 20 (TBS-T). Blocked membranes were incubated with primary antibody rabbit anti-dinitrophenylhydrazone, rabbit anti-3-nitrotyrosine or rabbit anti-4-hydroxynonenal (Alpha Diagnostic Intl. Inc.). After washing, membrane were then incubated with goat anti-rabbit alkaline phosphatase conjugated secondary antibody. Membranes were developed using 5-bromo-4-chloro-3-indolylphosphate dipotassium (BCIP) and nitro blue tetrazolium chloride (NBT) (Thermo Fisher Scientific) in alkaline phosphatase activity buffer (100mM Tris-HCl, 100mM NaCl, 10mM MgCl₂, pH 9.5). Dried membrane were scanned and image analysis was performed using Image Lab™ (Bio-Rad laboratories, Inc.).

Statistical analysis

Data are reported as means \pm SD; statistical analyses were performed using Student's t test. Differences were considered significant when $p \leq 0.05$.

Results

Oxidative stress markers in mice plasma and brain after ABT199 acute treatment

Among the other effects, oxidative stress in plasma and tissues is expressed by protein oxidation and lipid peroxidation. Protein carbonyls and 3-Nitrotyrosine (3-NT) are used as markers of protein oxidation, while protein-bound 4-hydroxy-2-nonenal (HNE) is a marker for lipid peroxidation [184], [185]. Protein carbonyls are the consequence of several processes due to free radicals reactions with proteins, some of which are: cleavage of the peptide backbone to produce carbon radicals that react with oxygen; oxidation of specific protein side chains; and covalent modification, via Michael addition, by reactive products of lipid peroxidation [186], [187]. 3-Nitrotyrosine is the result of the reaction of tyrosine residues with peroxynitrite (ONOO-) [188]. Lastly, HNE is produced from a lipid acyl chain (e.g. arachidonic acid) hydroperoxide. The hydroperoxide is formed following free radical attack on allylic H atoms of the acyl chains. HNE, one of the reactive alkenals produced, forms covalent adducts with proteins, particularly on Cys, His and Lys residues, via Michael addition changing their structure and impairing their function [189]. The levels of those oxidative stress markers were investigated in plasma and brain of mice after 72h from acute treatment with ABT199 (100mg/Kg). As shown in Fig.1A, in both genders, the levels of all three markers do not significantly change in group treated with acute ABT199 compared to the vehicle treated group. The absence of alteration in oxidative stress markers levels is reported also in mice brain tissue (Fig.1B).

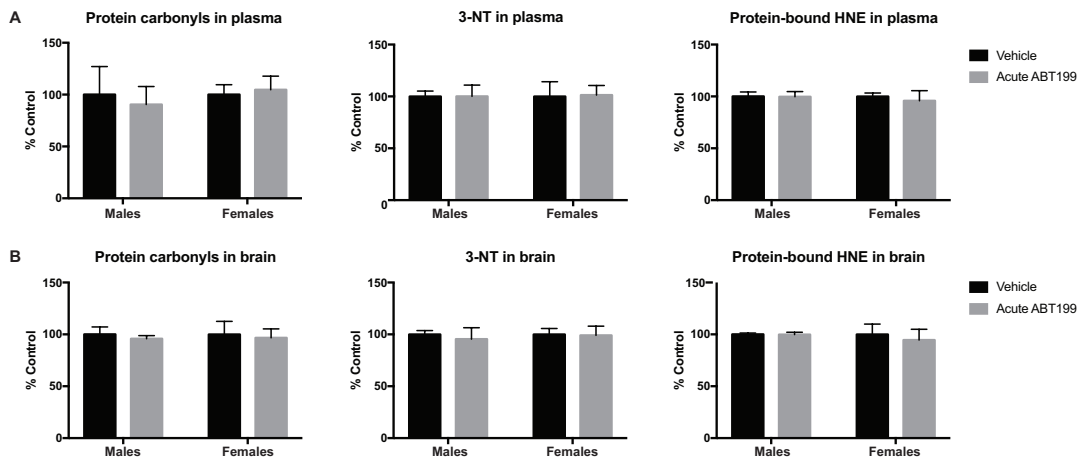


Figure 1. Oxidative stress markers levels in plasma (A) and in brain isolated from mice 72h after ABT199 acute treatment (100mg/Kg). The results show no significant differences between the levels of markers in the vehicle group and of the ABT199-treated groups. The mean value of Adj. Volume (Int) of subjects in vehicle group was taken as control 100%. $P < 0.05$; $n = 3-5$.

Oxidative stress markers in mice plasma and brain after ABT199 chronic treatment

The same oxidative stress markers (protein carbonyls, 3-NT and protein-bound HNE) were analyzed in plasma and brain of mice after 72h from the end of chronic treatment with ABT199 (100mg/Kg/d for 7 days). However, even after a prolonged treatment with this drug, the oxidative stress markers levels remain unaffected comparing the group treated with ABT199 for 7 days to the vehicle treated group of both genders (Fig.2).

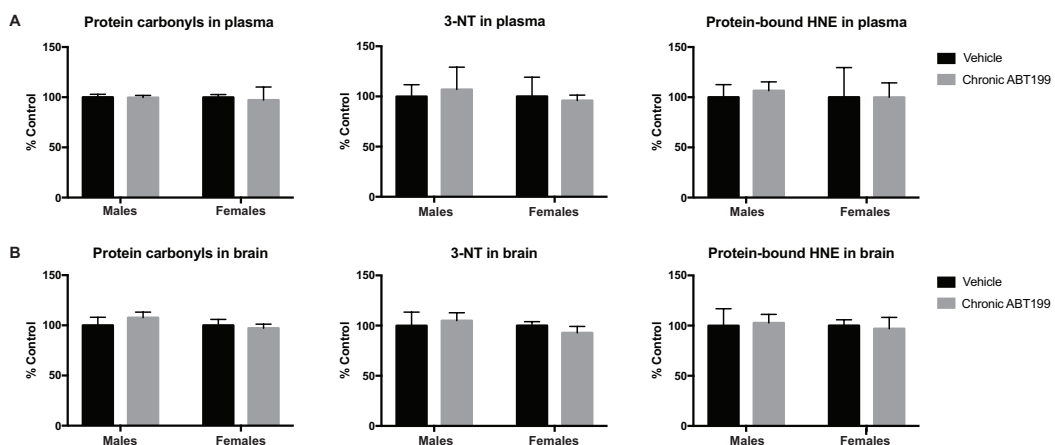


Figure 2. Oxidative stress markers levels in plasma (A) and in brain isolated from mice 72h after ABT199 chronic treatment (100mg/Kg/d for 7 days). The results show no significant differences between the levels of markers of the vehicle group and of ABT199-treated group. The mean value of Adj. Volume (Int) of subjects in vehicle group was taken as control 100%. $P < 0.05$; $n = 3-5$.

Behavioral test: Novel Object Recognition

The Novel Object Recognition (NOR) is one of the most used behavioral test to evaluate cognitive impairment in mouse model of CNS disorders. Particularly, it can be helpful because of the involvement in this simple recognition process of brain areas, such as the hippocampus and the frontal cortex, associated with memory and cognitive function. The mouse is allowed to explore an open field containing two identical object during the familiarization session. On the second session, one of the familiar objects is replaced with a novel one. This test is based simply on the natural, innate preference of a rodent to explore a novel object rather than a familiar one [183], [190]. The mice groups treated with both acute (100mg/Kg) (Fig.3A) and chronic (100mg/Kg/d for 7 days) (Fig.3B) ABT199, do not show any statistically significant impairment in memory cognition compared with the mice groups treated with vehicle (Fig.3).

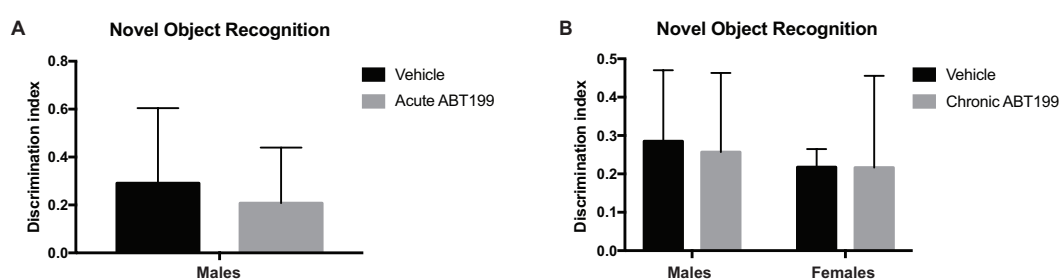


Figure 3. Novel Object Recognition (NOR) behavioral test on mice treated orally with vehicle or ABT199. Data are reported as Discrimination Index (DI), which allows to highlight the discrimination between the novel and the familiar objects. $DI = (TN - TF) / (TN + TF)$; TN=time spent exploring the novel object, TF= time spent exploring the familiar object A) NOR test on male mice group treated with vehicle compared to acute ABT199 (100mg/Kg) treated one. $n = 10$; $p < 0.05$. B) NOR test on both genders

mice groups treated with vehicle compared to chronic ABT199 (100mg/Kg/d for 7 days) treated one. n=3-5; p<0.05.

Future perspectives

In order to confirm that the Venetoclax does not induce oxidative stress in mice plasma and brain, it could be useful to investigate the oxidative stress markers levels after:

- an acute treatment with ABT199 dose higher than 100mg/Kg
- a longer chronic treatment with ABT199, for example 100mg/Kg/d for 21-28 days, which is the usual duration of treatment in lymphoid malignancies mice models [191], [192].

It might be interesting also to analyze the oxidative stress markers levels after the treatment with different targeted drugs to determine if other members of this new generation of anticancer agents can be associated with the risk to develop CICI.

Bibliography

- [165] R. B. Raffa, "A proposed mechanism for chemotherapy-related cognitive impairment (chemo-fog)," *J. Clin. Pharm. Ther.*, vol. 36, no. 3, pp. 257–259, Jun. 2011.
- [166] H. C. F. Moore, "An overview of chemotherapy-related cognitive dysfunction, or 'chemobrain,'" *Oncol. Williston Park N*, vol. 28, no. 9, pp. 797–804, Sep. 2014.
- [167] B. C. McDonald and A. J. Saykin, "Alterations in brain structure related to breast cancer and its treatment: chemotherapy and other considerations," *Brain Imaging Behav.*, vol. 7, no. 4, pp. 374–387, Dec. 2013.
- [168] M. Simó, X. Rifà-Ros, A. Rodriguez-Fornells, and J. Bruna, "Chemobrain: a systematic review of structural and functional neuroimaging studies," *Neurosci. Biobehav. Rev.*, vol. 37, no. 8, pp. 1311–1321, Sep. 2013.
- [169] T. A. Ahles and A. J. Saykin, "Candidate mechanisms for chemotherapy-induced cognitive changes," *Nat. Rev. Cancer*, vol. 7, no. 3, pp. 192–201, Mar. 2007.
- [170] A. M. Gaman, A. Uzoni, A. Popa-Wagner, A. Andrei, and E.-B. Petcu, "The Role of Oxidative Stress in Etiopathogenesis of Chemotherapy Induced Cognitive Impairment (CICI)-"Chemobrain"," *Aging Dis.*, vol. 7, no. 3, pp. 307–317, May 2016.
- [171] D. B. Zorov, M. Juhaszova, and S. J. Sollott, "Mitochondrial reactive oxygen species (ROS) and ROS-induced ROS release," *Physiol. Rev.*, vol. 94, no. 3, pp. 909–950, Jul. 2014.
- [172] E. J. Lesnefsky, S. Moghaddas, B. Tandler, J. Kerner, and C. L. Hoppel, "Mitochondrial dysfunction in cardiac disease: ischemia–reperfusion, aging, and heart failure," *J. Mol. Cell. Cardiol.*, vol. 33, no. 6, pp. 1065–1089, Jun. 2001.
- [173] R. K. Chaturvedi and M. Flint Beal, "Mitochondrial diseases of the brain," *Free Radic. Biol. Med.*, vol. 63, pp. 1–29, Oct. 2013.
- [174] G. Joshi et al., "Free radical mediated oxidative stress and toxic side effects in brain induced by the anti cancer drug adriamycin: insight into chemobrain," *Free Radic. Res.*, vol. 39, no. 11, pp. 1147–1154, Nov. 2005.
- [175] C. D. Aluise et al., "2-Mercaptoethane sulfonate prevents doxorubicin-induced plasma protein oxidation and TNF- α release: implications for the reactive oxygen species-mediated mechanisms of chemobrain," *Free Radic. Biol. Med.*, vol. 50, no. 11, pp. 1630–1638, Jun. 2011.
- [176] J. Tangpong et al., "Adriamycin-induced, TNF-alpha-mediated central nervous system toxicity," *Neurobiol. Dis.*, vol. 23, no. 1, pp. 127–139, Jul. 2006.
- [177] G. Joshi et al., "Alterations in brain antioxidant enzymes and redox proteomic identification of oxidized brain proteins induced by the anti-cancer drug adriamycin:

- implications for oxidative stress-mediated chemobrain,” *Neuroscience*, vol. 166, no. 3, pp. 796–807, Mar. 2010.
- [178] J. Tangpong et al., “Adriamycin-mediated nitration of manganese superoxide dismutase in the central nervous system: insight into the mechanism of chemobrain,” *J. Neurochem.*, vol. 100, no. 1, pp. 191–201, Jan. 2007.
- [179] J. Chandra, “Oxidative stress by targeted agents promotes cytotoxicity in hematologic malignancies,” *Antioxid. Redox Signal.*, vol. 11, no. 5, pp. 1123–1137, May 2009.
- [180] S. Cory, A. W. Roberts, P. M. Colman, and J. M. Adams, “Targeting BCL-2-like Proteins to Kill Cancer Cells,” *Trends Cancer*, vol. 2, no. 8, pp. 443–460, 2016.
- [181] A. W. Roberts et al., “Targeting BCL2 with Venetoclax in Relapsed Chronic Lymphocytic Leukemia,” *N. Engl. J. Med.*, vol. 374, no. 4, pp. 311–322, Jan. 2016.
- [182] A. Roberts and D. Huang, “Targeting BCL2 With BH3 Mimetics: Basic Science and Clinical Application of Venetoclax in Chronic Lymphocytic Leukemia and Related B Cell Malignancies: Basic science and clinical application of venetoclax,” *Clin. Pharmacol. Ther.*, vol. 101, no. 1, pp. 89–98, Jan. 2017.
- [183] M. Leger et al., “Object recognition test in mice,” *Nat. Protoc.*, vol. 8, no. 12, pp. 2531–2537, Dec. 2013.
- [184] G. Joshi et al., “Free radical mediated oxidative stress and toxic side effects in brain induced by the anti cancer drug adriamycin: Insight into chemobrain,” *Free Radic. Res.*, vol. 39, no. 11, pp. 1147–1154, Jan. 2005.
- [185] C. D. Aluise, D. St. Clair, M. Vore, and D. A. Butterfield, “In vivo amelioration of adriamycin induced oxidative stress in plasma by gamma-glutamylcysteine ethyl ester (GCEE),” *Cancer Lett.*, vol. 282, no. 1, pp. 25–29, Sep. 2009.
- [186] D. A. Butterfield and E. R. Stadtman, “Chapter 7 Protein Oxidation Processes in Aging Brain,” in *Advances in Cell Aging and Gerontology*, vol. 2, P. S. Timiras and E. E. Bittar, Eds. Elsevier, 1997, pp. 161–191.
- [187] M. Fedorova, R. C. Bollineni, and R. Hoffmann, “Protein carbonylation as a major hallmark of oxidative damage: update of analytical strategies,” *Mass Spectrom. Rev.*, vol. 33, no. 2, pp. 79–97, Apr. 2014.
- [188] R. Radi, “Peroxynitrite, a stealthy biological oxidant,” *J. Biol. Chem.*, vol. 288, no. 37, pp. 26464–26472, Sep. 2013.
- [189] H. Esterbauer, R. J. Schaur, and H. Zollner, “Chemistry and biochemistry of 4-hydroxynonenal, malonaldehyde and related aldehydes,” *Free Radic. Biol. Med.*, vol. 11, no. 1, pp. 81–128, 1991.

- [190] B. Grayson, M. Leger, C. Piercy, L. Adamson, M. Harte, and J. C. Neill, "Assessment of disease-related cognitive impairments using the novel object recognition (NOR) task in rodents," *Behav. Brain Res.*, vol. 285, pp. 176–193, May 2015.
- [191] E. A. Punnoose et al., "Expression Profile of BCL-2, BCL-XL, and MCL-1 Predicts Pharmacological Response to the BCL-2 Selective Antagonist Venetoclax in Multiple Myeloma Models," *Mol. Cancer Ther.*, vol. 15, no. 5, pp. 1132–1144, 2016.
- [192] S. L. Khaw et al., "Venetoclax responses of pediatric ALL xenografts reveal sensitivity of MLL-rearranged leukemia," *Blood*, vol. 128, no. 10, pp. 1382–1395, Sep. 2016.

